Sensors & Diagnostics

TUTORIAL REVIEW

View Article Online
View Journal

Cite this: DOI: 10.1039/d4sd00364k

Recent progress in fluorescence-based chemosensing of pesticides

Giriraj Kalaiarasi, *[ab] Ananthu Shanmughan, [a] Yohaeswari Jegadeesan,[a] Mannanthara Kunhumon Noushija, [a] Alenthwar Vamshi Krishna, [a] Harsha Gangadharan,[a] Deivasigamani Umadevi*[a] and Sankarasekaran Shanmugaraju *[a]

Poisoning of agricultural products through the use of pesticides has created a high risk to the environment and human health. In recent years, substantial research has been devoted to replacing harmful chemical pesticides with naturally derived organic compounds and the safer detection of pernicious pesticide residues by selective and sensitive methods using suitable sensor systems has also been given equal priority. Among various sensing methods that are currently available, fluorescence-based sensing has acquired widespread acceptance and become a feasible technique for the trace analysis of pesticide residues due to several practical advantages. In this review article, we provide a systematic overview of the recent progress made in using fluorescence-based chemosensing of different classes of pesticides and their success in real-world applications. Various fluorescence chemosensors highlighted in this article are categorized based on their sensing propensity for a particular class of pesticides. In the initial section of the article, we have highlighted a detailed discussion on the classification of pesticides, and various methods available for pesticide detection, and the later sections report various chemosensors reported to date for sensing different classes of pesticides. Finally, we put forward a short discussion on the advantages and existing practical difficulties in employing fluorescent chemosensors for pesticide detection and also state the future perspective of this field toward developing practically useful sensing systems.

Received 9th December 2024,
Accepted 26th March 2025

DOI: 10.1039/d4sd00364k

rsc.li/sensors

[a] Department of Chemistry, Indian Institute of Technology Palakkad, Palakkad-678623, Kerala, India. E-mail: umadevi@iitpkd.ac.in, shanmugam@iitpkd.ac.in
[b] Department of Chemistry, Karpagam Academy of Higher Education, Coimbatore-641021, Tamil Nadu, India. E-mail: kalaiarasichemist@gmail.com

1. Introduction

A class of chemicals known as pesticides can eradicate, discourage, or manage pests that negatively impact plant growth.[1] Pesticides can be synthetic or natural and used to prevent weed growth while crops are produced and stored.[2] These pests include nematodes, plant pathogens, insects, mollusks, birds, rodents, fish, mammals, and other

Giriraj Kalaiarasi

Dr. Giriraj Kalaiarasi holds an M.Sc. in Chemistry and completed her Ph.D. in Inorganic Chemistry in 2018 at Bharathiar University, Coimbatore. She is working as an Assistant Professor at the Department of Chemistry, Karpagam Academy of Higher Education, India. Her research interests focus on the biological applications of coordination complexes, catalysis, and sensor works.

Ananthu Shanmughan

Mr. Ananthu Shanmughan is a Ph.D. student at the Indian Institute of Technology Palakkad. He holds an Integrated M.Sc. in Chemistry from IIRBS, Mahatma Gandhi University, Kottayam. His research primarily focuses on developing small-molecule fluorescence sensors and synthesizing luminescent organic polymers for detecting emerging organic pollutants.

microorganisms.[1,2] All insecticides, herbicides, rodenticides, and fungicides that affect certain pests are called pesticides.[3] According to a study by Savary *et al.*, pests have caused production losses of rice (25–41%), potatoes (8–21%), wheat

Yohaeswari Jegadeesan

Ms. Yohaeswari Jegadeesan obtained her B.Sc. in Chemistry from Fatima College, Madurai in 2021 and M.Sc. Chemistry from Thiagarajar College, Madurai in 2023. She is doing her Ph.D. in the Department of Chemistry at the Indian Institute of Technology, Palakkad. Her research interest focuses on the design and synthesis of metal–organic frameworks and coordination polymers for gas adsorption studies.

Mannanthara Kunhumon Noushija

Ms. Mannanthara Kunhumon Noushija received her B.Sc. in Chemistry from Government Victoria College, Palakkad, in 2018, followed by an M.Sc. in Chemistry from the Calicut University campus, Thenhippalam, in 2020. She is pursuing her Ph.D. in the Department of Chemistry at the Indian Institute of Technology Palakkad, where her research focuses on developing small molecule-based fluorescence chemosensors for detecting biologically significant analytes.

Alenthwar Vamshi Krishna

Mr. Alenthwar Vamshi Krishna received his BS-MS dual degree in Chemistry in 2019 from the Indian Institute of Science Education and Research (IISER), Pune. He is presently a Ph.D. scholar in the Department of Chemistry at the Indian Institute of Technology, Palakkad. His primary research interests are in the design of organic cathode materials for advanced energy storage systems.

Harsha Gangadharan

Ms. Harsha Gangadharan is currently a Ph.D. student in Chemistry at the Indian Institute of Technology Palakkad. She completed her M.Sc. in Chemistry at Calicut University campus, Thenhippalam, and her B.Sc. in Chemistry at NSS College Nenmara, Palakkad. Her research interests are macrocycle-derived organic polymers for task- specific sensing and removal of organic contaminants from water.

Deivasigamani Umadevi

Dr. Deivasigamani Umadevi received her Ph.D. in Chemistry from the Indian Institute of Chemical Technology (IICT), Hyderabad, India. She held postdoctoral positions at Trinity College Dublin in Ireland before joining the Indian Institute of Technology Palakkad where she is currently a DST-Women Scientist in the Department of Chemistry. Her research interests include the computational study of nanostructures and supramolecular materials for their applications in energy and the environment.

Sankarasekaran Shanmugaraju

Dr. Sankarasekaran Shanmugaraju received his Ph.D. in Inorganic Chemistry from the Indian Institute of Science (IISc), Bengaluru. In 2014, he moved to Trinity College Dublin, Ireland, as an Irish Research Council (IRC) postdoctoral fellow. In October 2018, he joined the Department of Chemistry as an assistant professor at the Indian Institute of Technology Palakkad. Since June 2023, he has been an associate professor in the same institution. His group's current research activities encompass the design and self-assembly formation of novel structures, functional materials, and porous polymers for their applications in emerging sustainable technologies.

(10–28%), maize (20–41%), and soybeans (11–32%) on a global scale.[4] Other substances classified as pesticides include growth regulators, chemical disinfectants, plant defoliants, and chemicals used in swimming pools.[5] The usage of pesticides dates back to the dawn of human civilization. An efficient method to remove pests was essential since civilizations have had to contend with the difficulty of growing and conserving food supplies while dealing with pest interference. Originally used as a fungicide, elemental sulfur was eventually replaced by sulfides, arsenic (As_2O_3), lead hydrogen arsenate ($PbHAsO_4$), and mercury to eradicate pests.[6,7] In recent years, pesticide use has globally increased by 15–20 times to improve agricultural productivity and profitability.[8] Despite their widespread usage in agriculture, pesticides are also used in non-agricultural settings, such as sports grounds, grass management, pet care, vegetation control in industries (roadways, railroads), and managing pests in buildings.[9,10] Continuous pesticide exposure and ingestion of pesticide-contaminated food have long-term negative effects on the ecosystem and human health. Pesticides have a variety of functions for each species and have caused harm by reacting with creatures that are not their intended target.[11–13] Indirect harm to non-target creatures can occur through changes to interactions between individual and bulk populations, or direct harm can occur through effects on gene expression, reproduction, behaviour, and life cycle.[14]

When pesticides enter the body of a person or an animal, they are digested, stored, eliminated, and built up as fat.[15] They cause neurological, endocrine, reproductive, respiratory, gastrointestinal, dermatological, and carcinogenic conditions.[11,16] In some circumstances, the extended exposure might be fatal.[17] While 80% of the pesticides penetrate the environment, just 0.1% are exposed to target organisms and carry out their actions.[18] Pesticide residues are usually present in water bodies, cooked foods, fruit juices, and animal feeds and cannot be eliminated by simple washing.[19–21] Concerns over the health consequences on children have grown after the finding that human breast milk contains chemical pesticide residues.[22,23] Dichlorodiphenyltrichloroethane, or DDT, was the most widely used pesticide in the 1940s until it was discovered to be carcinogenic and to have negative effects on the associated biota. As a result, it was outlawed globally.[24–32] Environmental impact quotient (EIQ) and environmental risk index measurements are typically used to assess pesticide toxicity.[33] Pesticides have multiple effects on soil, such as lowering microbial biomass, soil respiration, and natural nitrogen fixation.[34] By disrupting the natural exchange of information between leguminous plants and symbiotic microbes, pesticides can harm soil fertility and lower crop output.[35] The food chain is the source of the detrimental effects on human health. When pesticides reach the human body, they mimic and oppose hormones, resulting in hormonal imbalance, reproductive issues, a decline in immunity and IQ, and cancer development.[36,37] Nearly one million people have been afflicted with acute pesticide poisoning, with fatality rates ranging from 0.4% to 1.9%, according to the World Health Organization (WHO).[38] Additionally, prolonged use slows the development of pesticide resistance.

Discriminative sensing of pesticides is crucial and essential due to their harmful effects. Pesticides have been detected using different methods, including capillary electrophoresis, enzyme-linked immune absorbent tests, and chromatographic methods combined with mass spectrometry.[39–43] Traditional detection methods use capillary electrophoresis, enzyme-linked immune absorbent tests, and extremely complex chromatographic procedures in conjunction with mass spectrometry. The drawbacks of these instrumental procedures include their high cost, intricate methodology, and need for expert labor.[9] Therefore, a straightforward, efficient, and user-friendly approach must be created. Sensing technology is a sophisticated technique that allows on-site detection and is very practical and economical. This technique depends on the combined impact of the modifications seen in electrochemistry, fluorescence spectroscopy, Raman spectroscopy, and ultraviolet-visible spectroscopy.[5,44,45] However, this requires significant time and resources to monitor common pesticide exposure, which may restrict their ability to perform high-throughput experiments on sizable populations. Among them, fluorescence-based sensors are superior because they provide great selectivity, outstanding signal-to-noise ratios, and real-time sample analysis.

Given this, research in the area of fluorescence-based chemosensing has received a lot of interest.[46–48] In general, the use of 'turn-on' (enhancement) fluorescence sensors is more advantageous for sensing applications because the interactions between sensors and analytes can easily be visualized by the naked eye due to the significant enhancement in fluorescence emission intensities.[49] However, the straightforward design of 'turn-on' fluorescent sensors is complicated and it often demands a careful design strategy. Further, the real-time applications of fluorescence 'turn-on' sensors are insufficient due to the lack of reversibility, selectivity, and small Stokes shift.[50] In contrast, the design and sensor applications of 'turn-off' fluorescence sensors are explored to a greater extent. In particular, the use of 'turn-off' fluorescent sensors for the detection of various classes of pesticides is well studied.[51] Fluorescence-based chemosensing of pesticides has been achieved thus far through employing luminescent organic & hybrid polymers, metal-containing scaffolds, nanoparticles, and discrete macrocycles.[52] Mechanistically, the detection occurs *via* many pathways,[53–55] and the fluorescence "turn-off" response (quenching), which indicates the pesticide-induced decrease of fluorescence intensity, is commonly observed. Energy transfer between the pesticide and the sensor system may be the reason for the quenching of fluorescence emission intensity. Förster resonance energy transfer (FRET), photoinduced electron transfer (PET), electron exchange (EE),

and inner filter effect (IFE) are the four mechanisms responsible for this energy transfer.[56]

In FRET, the donor (fluorophore) and acceptor (analyte) molecules are placed at a Förster distance of 15–60 Å. When an excited fluorophore relaxes to the ground state, it transfers excited energy to the acceptor molecule that promotes it to the excited state. The reabsorption of excited energy by the acceptor molecule causes notable fluorescence quenching. The energy transfer is possible only when the fluorophore's emission spectrum overlaps with the analyte's absorption spectrum. The interaction between the fluorophore and analyte is greater when they are at a shorter distance.[56] In PET, when the photoexcited fluorophore relaxes to the ground state, the excited state energy of the fluorophore is transferred to the acceptor (analyte) molecule, which causes fluorescence emission quenching. For the enhanced energy transfer to occur, the frontier molecular orbitals of the fluorophore and analyte must be similar and the lowest-unoccupied molecular orbital (LUMO) of the analyte must be lower than the LUMO of the fluorophore.[56] The EE process involves the transfer of an electron from an excited fluorophore to the excited state of the acceptor molecule, leading to the fluorescence quenching of the fluorophore, while simultaneously an electron transfer from the ground state of the acceptor to the ground state of the fluorophore occurs. The electron transfer can be between two systems or parts of the same system, and EE is a short-range electron transfer process. In IFE, the reabsorption of emitted photons from the excited fluorophore by the other molecules in the samples causes fluorescence quenching. Fluorescence quenching is also possible if the sample absorbs the excitation light before it excites the fluorophore.

The pesticide classification according to distinct domains, a thorough explanation of the fluorescence-based chemosensing of various pesticide classes, the detection process, the detection limit, and their applications in real-world samples are all covered in detail in the following section of this article.

2. Classification of pesticides

Pesticides are different from one another in terms of their identity based on physical and chemical properties. In addition, each pesticide is formulated for a specific activity against a target group of pests. Without knowing its chemical structure and variation in physiochemical properties, pesticide detection is tedious. Therefore, pesticides must be systematically classified and grouped for designing suitable detection methods. Pesticides can be categorized based on chemical composition, target organism, mode of entrance & action, and source of origin. Pesticides can be of natural origin (biopesticides derived from plants, animals, and microorganisms) or synthetically made (*i.e.* chemical pesticides). Biopesticides offer high specificity to target pests, low toxicity, and are environment friendly. Biopesticides are subdivided into microbial pesticides, plant-incorporated protectants, and biochemical pesticides. Chemical pesticides are environment-polluting, non-specific, and found to act upon several non-targeted organisms.[36,57] Depending on the mode of entry, they are classified as systemic (mediated through plants and ability to transfer to untreated tissues, *e.g.* glyphosate), contact (entry only through physical contact with the pests, *e.g.* paraquat), stomach poisons (mouth as a mode of entry, *e.g.* malathion), fumigants (vapor producing pesticides, *e.g.* aluminum phosphide) and repellents (repel pests from treated areas, *e.g.* methiocarb).[36] Chemical composition-based classification of pesticides has been considered the most practical and relevant approach. This type of classification includes all classes of pesticides (insecticides, herbicides, rodenticides, and fungicides) and acts as evidence for their observed efficacy, and physical and chemical properties. Accordingly, there are five main categories of pesticides as described herein.[58]

Organochlorines are chlorinated hydrocarbons (chloroalkanes and chloroarenes) mostly containing five or more than five chlorine atoms (see Fig. 1 for structures). They are the early examples of pesticides used in agriculture.[6] Most of these chemicals have been applied as insecticides and structurally fall into five types – a) DDT and its structural analogues, b) hexachlorocyclohexane (HCH), c) cyclodienes, d) toxaphene, and e) mirex and chlordecone.[57] Owing to their high chemical stability, organochlorine pesticides accumulate in high concentrations in soil and severely affect human health through the food chain. For instance, the half-life period of DDT is about 15 years, and it remains in the body for more than 50 years.[59] It has been proven to accumulate in the adipose tissue and affect the central nervous system.[60] First, the nerve membranes get affected which then cause changes in the flow of K^+ and Na^+ ions through nerve cells.[57] This will lead to convulsions, acute poisoning, seizures, and paralysis in the later stage.[2]

Organophosphate pesticides are phosphoric acid esters (see Fig. 2 for structures) that exhibit action against several pests by exerting multiple functions. The use of organophosphate pesticides has increased steadily in recent years because of the impact on agricultural productivity and increased crop yields.[61,62] These biodegradable pesticides are comparatively less harmful environmental pollutants. However, in humans, they inhibit acetylcholine, an enzyme that disturbs

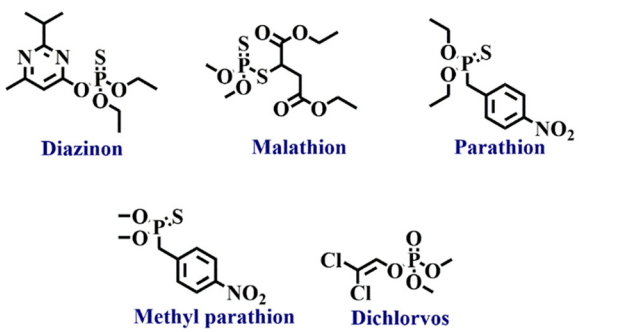

Fig. 1 The structures of organochlorine pesticides.

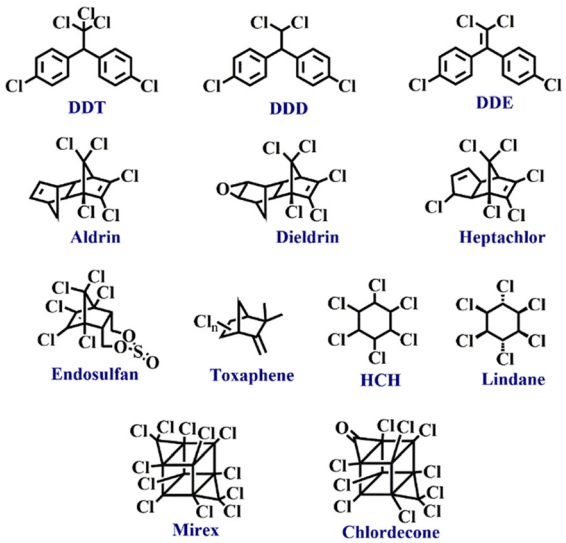

Fig. 2 The structures of organophosphate pesticides.

acetylcholinesterase neurotransmitters, which results in the failure of nerve impulses across the synapse, which could end up in paralysis.[63] Symptoms include headache, nausea, convulsions, cramps, loss of reactions, coma, and eventually death.[64,65] Another concern about using organophosphate is phosphate poisoning, which is in general treated mainly by intake of atropine, an anticholinergic drug.[66]

Another type of pesticide is carbamates, which are organic acid esters derived from carbamic acid (see Fig. 3 for structures). They are used as insecticides, herbicides, nematicides, and fungicides. Carbamates are short-lived and their toxicity generally coincides with the organophosphate's toxicity. Carbamates also disturb the activity of acetylcholinesterase and produce acute symptoms like cough, mitosis, cardiovascular and gastrointestinal effects, and illness associated with the central nervous system.[67,68] They pose minimal environmental pollution and can be degraded easily.[2,6]

Pyrethroids are naturally derived organic pesticides and due to their high demand, their derivatives can also be synthetically produced. Pyrethroids are generally used as insecticides (see Fig. 4 for structures).[2] Active components of these pesticides are pyrethrin I and pyrethrin II with small amounts of jasmolins and cinerins. Pyrethroids are less toxic to mammals

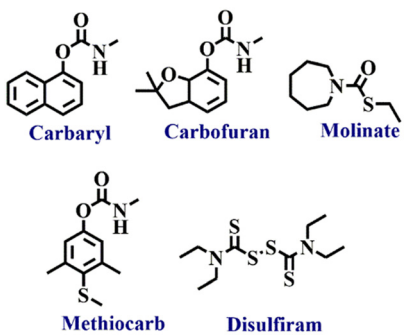

Fig. 3 The structures of carbamate pesticides.

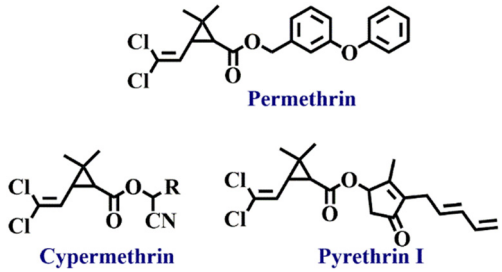

Fig. 4 The structures of pyrethroid pesticides.

and animals but comparatively toxic to insects and fish. Although insect pests absorb pyrethroids, their penetration power into soil and solubility in water are not very effective in affecting underground pests. Many commercial products like pet sprays, pet shampoos, mosquito repellents, and human head lice drugs contain pyrethroids.[69,70]

Another type of classification of pesticides is based on their target organism. Table 1 summarizes different pesticides classified according to their target pests and notable examples.

3. Various approaches for pesticide detection

The conventional detection of pesticides involves the utilization of different techniques including gas

Table 1 Classification of pesticides based on the target organism

Pesticides	Target pests	Example
Insecticides	Insects, arthropods	Aldicarb
Fungicides	Fungi	Azoxystrobin
Bactericides	Bacteria	Cu-complexes
Herbicides	Weeds, unwanted plants	Atrazine
Larvicides	Larva	Methoprene
Molluscicides	Molluscs	Metaldehyde
Nematicides	Nematodes	Aldicarb
Ovicides	Insect and mite eggs	Benzoxazine
Piscicides	Fish	Rotenone
Rodenticides	Rodents	Warfarin
Silvicides	Wood vegetation	Tebuthiuron
Termiticides	Termites	Fipronil
Virucides	Virus	Scytovirin
Avicides	Birds	Avitrol
Acaricides	Mites	Bifenazate
Algaecides	Algae	Copper sulfate
Desiccant	Plant tissues	Boric acid
Lampricides	Lamprey larva	Trifluoromethyl
Predacides	Mammal predators	Strychnine
Mothballs	Moth larvae, molds	Dichlorobenzene
Attractant	Wide range of pests	Pheromones
Insect growth regulator	Insects	Diflubenzuron
Defoliant	Plant foliage	Tribufos
Bait	Variety of organisms	Anticoagulants
Fumigant	Variety of organisms	Aluminum phosphide
Repellents	Range of pests	Methiocarb

chromatography (GC), high-performance liquid chromatography (HPLC), surface-enhanced Raman spectroscopy (SERS), accelerator mass spectrometry (AMS), and capillary electrophoresis (CE). However, the requirement of skilled manpower, sophisticated instrumental setup, and non-portability make these techniques not feasible for practical on-site sensing applications.[57,71,72] To tackle these difficulties, alternate detection methods were sought for relatively low cost, time-saving, and operational simplicity. As alluded to above, the use of fluorescent-based chemosensors for the selective detection of pesticides has taken a front lead and is of several categories.

Colorimetric sensors offer naked-eye determination of specific chemical compounds in pesticide residues. They provide an opportunity for on-site detection of real-time samples owing to their practical applicability and simplicity.[73–78] The colorimetric sensors work by inducing changes in the color and intensity of the absorption bands before and after pesticide addition.[79] Qualitative analysis of pesticide concentrations is possible by observing changes in the color, whereas recording UV-visible spectra of the resultant compounds permits quantitative analysis of pesticide residues.[80,81] Recent years have witnessed a flourishment of colorimetric sensors based on nanoparticles (NPs) for the detection of various classes of pesticides. In particular, NPs as sensors have been greatly seen in agricultural food analysis.[74–78,82,83] In certain cases, the application of NPs has provided a higher level of sensitivity than a chemical treatment method. For example, silver NPs wrapped with graphene oxide allowed for the detection of carbaryl pesticide at a lower limit of detection (LoD) between 0.1 and 50 ppm;[84] this level of sensitivity was found to be superior to that observed from an azo coupling reaction-based colorimetric probe.[85] Demonstration of a dual technology (smartphone-assisted and spectroscopic) has been reported with a nanoenzyme for the on-site detection of organophosphates.[86] Ghoto and his group have developed colorimetric probes for pesticide detection based on Cu (coated with cetyltrimethyl ammonium bromide) and Ag NPs (coated with sodium dodecyl sulfate) with LoD values of 97.9 and 9.1 ng ml^{-1}.[87,88] By employing an origami paper sensor, Bordbar *et al.* showed selective detection of organophosphate and carbamate pesticides in water, rice, and apple juice, and also reported detection in the vapor phase.[89,90]

Paper sensor-based detection methods have evolved from enzyme activity inhibition, mostly acetylcholinesterase (AChE) and butyrylcholinesterase (BChE). Inhibition of enzyme activity may be brought about by preventing acetylthiocholine, acetylcholine, and butyrylcholine from being converted to thiocholine, choline, and acetic acid by these enzymes. This interrupts the signaling and transmission of neuronal synapses. It is well-known that organophosphates effectively inhibit AChE. Consequently, this enzyme can be used as an indicator for organophosphate detection.[91,92] Organophosphate and carbamate contents in vegetables and fruits have been determined on-site by employing a double film screening card constructed from AChE and indoxyl acetate. The film detected phoxim in apples, lettuce, and cabbage between 5–20 μg mL^{-1}.[92] For the same class of pesticides, a biosensor based on AChE has been developed by the Badawy team, which worked based on the change in yellow coloration.[93] A similar probe was also developed and used for malathion detection with a LoD of 2.5 ppm within 5 min of incubation.[94]

The detection of pesticides has also been accomplished by the electrochemical method and is dependent on the working electrode (transducer). They work by producing an electrical signal due to the interaction of the target pesticides with the transducer. Sensitivity and selectivity can be improved by fabrication, surface modification, and enzyme immobilization.[95] For instance, polymers like poly(3,4-ethylenedioxythiophene) and carbon nanotubes were used to develop NP-modified electrodes, able to detect mancozeb (a fungicide) in water using cyclic voltammetry analysis (LoD = 10 μmol L^{-1}).[96] A similar approach with carbon nanosphere for the selective detection of carbofuran, carbaryl, fenobucarb, and isoprocarb in corn and wheat samples has been reported.[97] MXene-carbon nanohorns, silicon carbide, and CuO nanocomposite-derived electrodes have been designed to serve this purpose.[98–102] Fabrication methods for electrochemical sensors include thin film and thick film technologies. Thin films are relatively costly due to the application of lithographic technology but show high reproducibility. Thick films use cost-effective techniques like inkjet printing, 3D printing, and screen printing. Printed electrodes have different electroanalytical performances and possess varying catalytic abilities, composition, and specificity for samples being analyzed.[103–108]

Fluorescence-based sensing is one of the widely used methods for pesticide detection. They display their action by decreasing or increasing the sensor emission intensity after mixing pesticides and the method depends on the sample concentration.[109] Many reports have shown that the pesticides act as fluorescent quenchers.[110] Small molecule pesticide samples could be analyzed with conjugated polymers as sensors. Recently, the use of conjugated polymers in solution has been reported for targeted two-photonic excitation, and these polymers have been incorporated within carbon nanotubes.[111,112] NPs derived from luminescent polymers combined with Au NPs were found to detect paraoxon by quenching the initial fluorescence intensity. This combination has practical application in analyzing real-time lake water and cabbage extracts.[113] A europium coordination polymer was used to detect fipronil in European eggs in solution and a paper strip-based sensor by the fluorescence quenching mechanism. Interestingly, this sensor was so selective that other pesticide samples with structurally similar analogues induced no change in the emission intensity.[114,115] Also, discrete macrocycles with different photophysical properties have been employed to detect pesticides. Fluorescent macrocycles can be built through supramolecular

architecture by attaching themselves to a non-fluorescent macrocycle[116] or by the covalent binding of two or more macrocycles to a fluorescent linker. Dithianon has been detected by a covalent linker bound with two cyclodextrins.[117] The sensor ability was mainly due to the interaction between the signalling element of the macrocycle and the pesticide sample, which can fit well enough into the macrocycle cavity.[118] In addition, quantum dots (*e.g.* carbon quantum dots),[119,120] nanocrystals (*e.g.* cadmium sulfide nanocrystals),[121,122] and metal–organic frameworks (MOFs) have been found effective as fluorescent sensors.[123,124]

After reviewing the previously described methods, environmental and analytical chemists have created effective fluorescence sensing approaches for pesticide detection. Among the various detection strategies adopted for pesticide detection in environmental samples, agriculture, food safety, and quality control, the fluorescence-based detection method plays a vital role due to its low cost, appropriateness for quick pesticide detection screening procedures, and target molecule specificity and sensitivity. Moreover, this method makes it feasible to obtain high-quality image data. Importantly, this method exhibits good pesticide residue sensing performance and its simplicity makes fluorescence-based sensing a well-suited method for pesticide detection.

4. Fluorescence-based chemosensing of pesticides

The design and development of fluorescent-based chemosensors for detecting environmental pollutants and hazardous substances have significantly increased in recent years. In light of this, several fluorescent chemosensors have been reported for pesticide detection. In this section of the review, we have exemplified in detail a variety of fluorescent chemosensors utilized for the selective detection of various classes of pesticides. Besides, the synthesis and properties of sensors, pesticide detection mechanisms, and sensitivity have also been mentioned.

4.1 Fluorescence sensing of organophosphate (OPP) pesticides

Organophosphate (OPP) pesticides have been used extensively to increase agricultural output. However, higher concentrations of OPPs are detrimental to the environment, human health, and other organisms. Numerous ways, such as percutaneous absorption, inhalation, and ingestion from air, water, sediment, and crops, introduce OPPs to living things. OPPs can easily damage soil, aquatic life, and other living things because of their high adsorption capacity and increased water solubility.[125] An estimated 100 different OPPs have been created for commercial usage. The first OPP that was created with agricultural insecticidal properties was hexaethyl tetraphosphate.[126,127] Various categories of OPPs are given in Fig. 5. While OPPs undeniably contribute to substantial increases in agricultural productivity, their

Fig. 5 Examples of various organophosphate pesticides.

adverse effects on human health and the environment have emerged as an enormous challenge to society and the natural world. As a result of the serious contamination by OPPs, it has become crucial to develop sensors capable of detecting OPPs in soil, air, fruits, vegetables, beverages, and more.[128–130] Due to the extensive literature reports on the detection of OPPs, we aimed herein to compile only the fluorescent-based chemosensors used for various types of organophosphate detection. Table 2 summarizes the sensing properties of different fluorescence sensors employed for detection of various OPPs.

Phosphate detection. Phosphates are the ester form of phosphoric acid and their general formula is $(OR_3)P{=}O$. Different types of fluorescence sensors were designed and used for phosphate detection. For example, graphene quantum dots (G-QDs) in conjunction with the AChE enzyme were employed to detect paraoxon with a good sensitivity for detection.[130] As an effective AChE inhibitor, paraoxon induced a notable fluorescence quenching by forming aggregates. The half-maximum inhibitor concentration (IC_{50}) was determined to be 19.86 nM and the LoD was 2 nM. In another study, Peng and coworkers reported the microwave-assisted synthesis of magnesium and nitrogen co-doped carbon dots, Mg,N-CDs.[131] Mg,N-CDs displayed blue emission and good solution processability. The fluorescent sensing probe was designed by mixing Mg,N-CDs with pralidoxime (PAM, a medicine used to treat phosphate poisoning) as a linker. Mg,N-CDs in the presence of PAM exhibited good fluorescence 'turn-off' sensing responses for paraoxon pesticides (Fig. 6). In this method, PAM enabled the electron transfer mechanism from Mg, N-CDs to paraoxon resulting in fluorescence emission quenching. The LoD value was reported to be 0.87 nM and Mg,N-CDs displayed selective sensing responses even in the presence of interfering analytes. The sensing studies were further demonstrated using real-water samples.

A luminescent nanoparticle aggregate was developed from an amphiphilic luminescent polymer in an aqueous buffer medium and it was combined with gold nanoparticles to produce the aggregate-based sensing probe (PTDNPs), which was used for paraoxon detection through the analyte-induced dis-aggregation mechanism.[113] Interestingly, the luminescent

Table 2 Summary of fluorescence sensing properties of various sensors for organophosphate pesticide detection (other class analytes are mentioned to highlight the selectivity of sensors)

Sensors	Analytes	LoD	Ref.
Graphene quantum dots (GQDs)	Paraoxon	2 nM	130
Mg,N-CD-PAM	Paraoxon	0.87 nM	131
AIE nanoparticles (PTDNPs)	Paraoxon	0.38 ng ml^{-1}	113
{$(Ru(bpy)_3)^{2+}$-ZIF-90)} and MnO_2 NSs	Methyl parathion	0.037 ng mL^{-1}	132
L-tyrosine methyl ester functionalized carbon dots (Tyr-CDs)	Methyl parathion	4.8×10^{-11} M	133
CdTe-QDs/CTAB	Methyl parathion	18 ng mL^{-1}	134
Carbon dots	Paraoxon-ethyl	0.22 μM	135
NS-Cdots	Dichlorvos	5.0×10^{-10} M	136
CdTe quantum dots (QDs)	Chlorpyrifos	~0.1 nM	137
Gold-based nanobeacon	Isocarbophos, profenofos, phorate and omethoate	0.35 μM	138
Cu(II) complexes of 8-((*E*)-((thiophen-2-yl)methylimino) methyl)-7-hydroxy-4-methyl-2*H*-chromen-2-one	Azamethiphos	55 nM	139
Supramolecular structure-based fluorescent sensor Eu-IRMOF-3-EBA	Prothiofos and profenofos	0.0018 ppb	140
Up-conversion fluorescent nanoparticles-gold nanoparticles	Malathion	1.42 nM	141
Eu(III)-complex of bathophenanthroline	Azinphos, ethyl malathion, and heptachlor	0.68 μM (azinphos), 0.92 μM (ethyl malathion) and 0.35 μM (heptachlor)	142
AgNPs-β-cyclodextrins hybrid material @ 2,3-dihydro-5-oxo-5-*H*-thiazolo[3,2-a]pyridine-7-carboxylic acid	Malathion	0.01 μg mL^{-1}	143
Rhodamine B (RB) functionalized AuNPs	Dimethoate	0.004 ppm	144
AgNPs/oxMWCNTs	Dimethoate	0.003 μg mL^{-1}	145
Dithizone (DZ)-CdTe QDs	Dimethoate	0.005 μg mL^{-1}	146
Molecularly imprinted polymer-CDs	Dimethoate	1.83×10^{-11} mol L^{-1}	147
RB-Ag NPs	Fenamithion	10.000 nM	148
1,8-Naphthalimide dye, quaternary ammonium salt with a boronate group	Trichlorfon, methyl parathion, and acephate	4.72×10^{-9} g L^{-1}, 3.36×10^{-10} g L^{-1} and 1.16×10^{-9} g L^{-1}	149
2-Amino terephthalic acid co-coordinated Co-MOF complex	Bis(*p*-nitrophenyl) phosphate (BNPP) and nitrophenyl phosphate (PNPP)	352 nM (PNPP)	150
CdSe@SiO_2@MIP	Parathion-methyl	0.004 mg kg^{-1}	151
$NaYF_4$:Yb, Er up-conversion NPs combined with Au Nps	Parathion-methyl, monocrotophos, and dimethoate	0.67 ng L^{-1}	152
Surface molecularly imprinted CdTe nanoparticles	Parathion	0.218 μmol L^{-1}	153
N-doped carbon dots (NCD)	Methyl parathion	0.338 μmol L^{-1}	154
$CuInS_2$-QDs and Pb(II)	Methyl parathion	0.06 μmol L^{-1}	155
Eu(III) complexes containing 4-hydroxy benzylidene imidazolinone with nitrogen-containing heterocyclic 1,10-phenanthroline	Methyl parathion	95 nM	156
ZnPO-MOF containing 1,2,4,5-tetrakis(4-carboxyphenyl) benzene	Methyl parathion	0.456 nM	157
Zirconium MOF appended 1,2,4,5-tetrakis(4-carboxyphenyl)benzene	Methyl parathion	0.438 nM	158
Europium(III) complexes containing amino-substituted β-cyclodextrin	Fenitrothion	1×10^{-12} M	159
Europium-8-allyl-3-carboxy coumarin (Eu(III)-ACC)	Chlorpyrifos, crotoxphos, and endosulfan	6.53 μmol L^{-1} for chlorpyrifos, 0.004 μmol L^{-1} for endosulfan and 3.72 μmol L^{-1} for crotoxyphos	160
Europium-doped titanium oxide nano-powder	Chlorpyrifos	3.2×10^{-11} mol L^{-1}	161
Mn(II)-doped ZnS quantum dots coated with an acrylamide-based MIP	Chlorpyrifos	0.89 μM	162
Plant-based green carbon dots	Diazinon, glyphosate, and amicarbazone	0.25, 0.5, and 2 ng mL^{-1}	163
L-cysteine capped CdS-QDs/DF20	Diazinon	0.13 nM	164
Tb(III)-complex of 3-ally-salicylohydrazide	Dichlorvos	1.183 μM	165
Hg(II) complex of novel cholesterol derivative, 4-chloro-7-nitro-1,2,3-benzoxadiazole (CTN) using triazole as a linker	Dichlorvos, glyphosate, chlorpyrifos, diazinon, and phoxim	0.015, 0.018, 0.087, 0.098, and 0.113 μg mL^{-1}	166
Biginelli derivatives of cobalt complexes	Malathion, azamethiphos	9.2 nM and 11 nM	167
Picolyl-functionalized rhodamine derivative	Glyphosate	4.1 nM	168
p-tert-butylcalix[4]arene	Glyphosate	7.91×10^{-7} M	169
Carbon dots + Fe(III)	Glyphosate	8.75 ppb	170
CDs with AgNPs (CDs/AgNPs)	Glyphosate.	12 ng mL^{-1}	171

Table 2 *(continued)*

Sensors	Analytes	LoD	Ref.
Zr-MOF, Fe_3O_4@SiO_2@UiO-67	Glyphosate	0.093 mg L^{-1}	172
CdTe quantum dots capped with thioglycolic acid (TGA-CdTe-QDs) and gold nanoparticles stabilized with cysteamine (CS-AuNPs)	Glyphosate	9.8 ng kg^{-1}	173
2D MOF nanosheets with calix[4]arenes	Glyphosate	2.25 μM	174

nanoparticle aggregates could identify paraoxon even in polluted lake water and cabbage extracts with a recovery efficiency of up to 93%. The LoD value was calculated to be 0.38 ng mL^{-1}, a comparable level to various other sensors exemplified herein. Another group reported an interesting fluorescence probe (P5C10) based on a coumarin fluorophore which was directly attached to a pillar[5]arene core to sense methyl parathion with high affinity (2.38×10^{-4} M^{-1}).[175] It was demonstrated that P5C10 forms a selective 1:1 host–guest complex with methyl paraoxon through π–π stacking interactions, while other analytes displayed poor host–guest complexation with P5C10. The association constant was determined to be 2.38×10^4 L mol^{-1}. In another study, Li *et al.* developed a novel MOF-based sensing platform that consists of a $Ru(bpy)_3^{2+}$-ZIF-90-MnO_2 to detect methyl parathion with a wide concentration range of 0.050–60 ng mL^{-1} and with a LoD of 0.037 ng mL^{-1}.[132] The visual color changes also indicated the high selectivity of $Ru(bpy)_3^{2+}$–ZIF-90–MnO_2 for methyl parathion. The team led by Ai and Mang reported a simple, sensitive fluorescence probe Tyr-CDs for methyl parathion detection.[133] The probe Tyr-CDs are carbon dots functionalized with L-tyrosine methyl ester (Tyr-CDs) and the tyrosinase system. The fluorescence emission of carbon dots was quenched by the quinone produced by the oxidation of tyrosine methyl ester by tyrosinase enzyme. However, the presence of methyl parathion inhibited the enzyme activity and thus reduced the rate of fluorescence quenching. It was found that the enzyme inhibitory activity was linearly related to the concentrations of methyl parathion and the LoD value was determined to be 4.8×10^{-11} M. The selective sensing was further successfully explored in cabbage, milk, and fruit juice samples.

Meanwhile, that year (2015) Yan *et al.* developed a sensitive fluorescence probe, mercaptopropionic acid (MPA)-capped CdTe-QDs for detecting methyl parathion showing a detection limit of 18 ng mL^{-1}. In this study, the probe works based on the electron transfer phenomenon that takes place between (MPA)-capped CdTe-QDs and *p*-nitrophenol (a product formed from hydrolysis of methyl parathion by OPH) in cetyltrimethylammonium bromide (CTAB) and the electron-deficient *p*-nitrophenol gets absorbed on the electronegative MPA-capped CdTe-QDs through strong hydrophobic interactions. As a result, the fluorescence of the probe was quenched.[134] By combining double QDs with nanoporphyrin (QDs-nanoporphyrin), a paper-based fluorescence visualization sensor was developed and used to detect dichlorvos, demeton, and dimethoate by using it through a "turn-off-on" detection mode.[176] In 2017, Chang *et al.* reported the synthesis of fluorescence carbon dots through simple acid carbonization of sucrose in-house.[135] This has been used to detect paraoxon-ethyl with a LoD of 0.220 ± 0.020 μM. Additionally, Hu *et al.* created an effective fluorescent probe that emits blue fluorescence, such as nitrogen and sulfur co-doped CDs (NS-Cdots), to detect OPs-dichlorvos (DDVP) in Chinese cabbage samples (Fig. 7 for details).[136] The observed LoD was 5.0×10^{-10} M.

Phosphorothioates. Examples of phosphorothioates are malaoxon, prefonofos, omethoate, and azamethiphos. These substances serve distinct fundamental purposes in safeguarding crops as insecticides and are employed as antiparasitic medication in aquaculture.[177] Zhang *et al.* reported a simple method for the development of fluorescence turn-on chemosensors using CdTe quantum dots for the detection of organophosphorothioate pesticides (Fig. 8).[137] CdTe QDs exhibited green emission and experienced a strong quenching of emission intensity *via* the

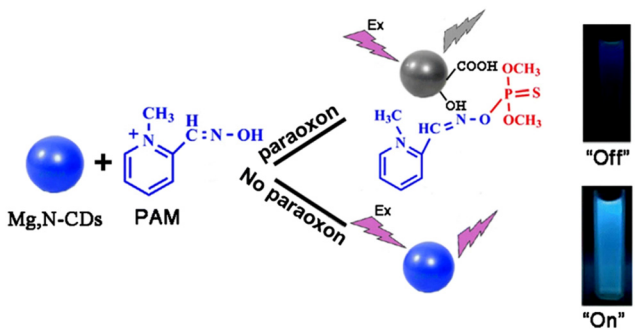

Fig. 6 Fluorescence 'turn-off' sensing of paraoxon using the Mg,N-CDs probe through electron transfer from PAM to paraoxon. Reprinted with permission from ref. 131. Copyright 2018 Springer Nature.

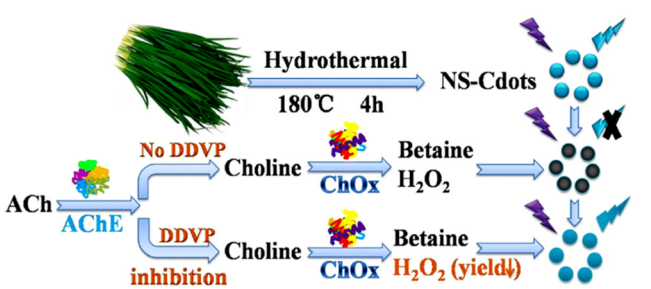

Fig. 7 Schematic representation of fluorescence turn-off-on based sensing of OPs-dichlorvos (DDVP). Reprinted with permission from ref. 136. Copyright 2019 Springer Nature.

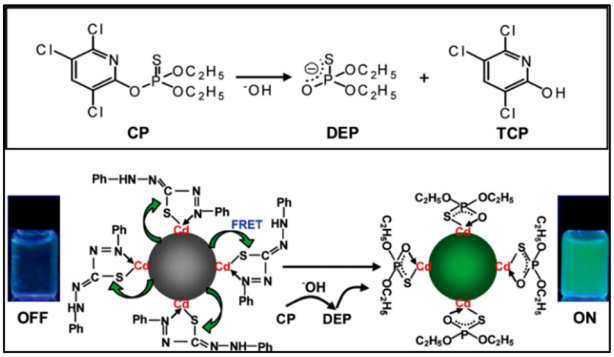

Fig. 8 Hydrolysis of chlorpyrifos (CP) to diethylphosphorothioate (DEP) and trichloro-2-pyridinol (TCP) in a basic medium (above). The fluorescence of CdTe QDs was quenched by the coordination of dithizone on the surface of CdTe QDs. The fluorescence emission of CdTe QDs was subsequently restored due to the replacement of dithizone by the DEP ligand (below). Reprinted with permission from ref. 137. Copyright 2010 American Chemical Society.

FRET mechanism when combined with dithizone due to the binding of dithizone to the surface of CdTe quantum dots in alkaline media. The introduction of organophosphorothioate resulted in the displacement of dithizone on the surface of CdTe QDs by the hydrolysis product of the organophosphorothioate, leading to the enhancement of fluorescence and the LoD for chlorpyrifos was as low as ~0.1 nM. Notably, the fluorescence turn-on chemosensor directly detects chlorpyrifos residues in apples with a detection limit of 5.5 ppb.

In 2015, Dou *et al.* developed a fluorescence assay based on a gold-based nanobeacon probe to detect various OPPs such as isocarbophos, profenofos, phorate, and omethoate.[138] Under optimized conditions, this method was fast and highly responsive for the concentration limit of 0.035 μM, 0.134 μM, 0.384 μM, and 2.35 μM for isocarbophos, profenofos, phorate, and omethoate, respectively. Additionally, this technique can detect trace amounts of organophosphorus pesticides in real substances. The detection of azamethiphos has been done by Bhasin *et al.* using a MOF-based fluorescent chemosensor such as Cu(II) complexes of 8-((*E*)-((thiophen-2-yl)methylimino) methyl)-7- hydroxy-4-methyl-2*H*-chromen-2-one in aqueous medium.[139] Abdelhameed and team reported the sensing nature of the supramolecular structure-based fluorescent probe Eu-IRMOF-3-EBA, which was synthesized by modifying IRMOF-3 with ethylbenzoylacetate and then coordinating it with Eu(III) ions. The supramolecular structure exhibited robust fluorescence emission in the near-infrared range, which significantly diminished upon prothiofos and profenofos exposures.[140]

Phosphorodithioates. Phosphorodithioates have been extensively used to control insects. Additionally, it can be used to keep animals at home to manage ticks and insects, including fleas and ants. Chen *et al.* reported a self-assembled supramolecular probe for phosphorodithioate detection using a conjugated polymer.[141] The sensor was designed by combining a negatively charged gold nanoparticle with a cationic-conjugated organic polymer. The self-assembled supramolecular probe was used to sense malathion with a 1.42 nM detection limit. Moreover, the sensor demonstrated an effective detection of malathion in tap water that had been tampered with, as well as in matcha samples, with a high level of precision. An MOF-based fluorescent sensor such as the Eu(III) complex of bathophenanthroline was reported to detect several pesticides such as heptachlor, azinphos ethyl, and malathion.[142] These pesticides attenuated the fluorescence emission of the sensor at λ = 614 nm. The respective detection limits in acetonitrile were 0.68 μM, 0.92 μM, and 0.35 μM. Wang *et al.* reported an off–on fluorescent sensor for detecting malathion.[143] By combining the AgNPs-β-cyclodextrin hybrid material and 2,3-dihydro-5-oxo-5*H*-thiazolo[3,2-*a*]pyridine-7-carboxylic acid (TPCA), they have observed the fluorescent quenching of TPCA at λ = 420 nm based on the FRET mechanism. Malathion was found to bind with AgNPs-β-cyclodextrins, resulting in TPCA release, thereby recovering the probe fluorescence emission. The detection limit was 0.01 μg mL^{-1}. A selective and effective fluorescent turn-on sensor consisting of rhodamine B (RB) functionalized AuNPs was developed for dimethoate detection in water and fruit samples. It was proposed that the sensing follows the FRET mechanism.[144] AuNPs suppressed the fluorescence of RB, but when OPPs were introduced, the fluorescence was restored as RB molecules on the surface of AuNPs were displaced by OPPs. The LoD for OPPs was reported to be 0.004 ppm.

Hsu *et al.* synthesized a novel turn-on fluorescent sensor based on silver-nanoparticles-modified oxidized multiwalled carbon nanotubes (AgNPs/oxMWCNTs) which has a peroxidase-like activity to detect dimethoate in lake water and fruits.[145] The presence of dimethoate inhibits the catalytic activity of AgNPs/oxMWCNTs because of the contact between dimethoate and AgNPs. This interaction caused a decrease in fluorescence, and the LoD was determined to be 0.003 μg mL^{-1}. Sheng *et al.* developed the dithizone (DZ)-CdTe QDs fluorescent quenching system for FRET-based detection of dimethoate.[146] After mixing dimethoate (DMT), the dithizone molecule was removed from the surface of the quantum dots (QDs), which restored the fluorescence in the CdTe QDs. The minimum detectable concentration using this technique was 0.005 μg mL^{-1}. Another interesting sensor based on a molecularly imprinted polymer was developed for dimethoate detection *via* the FRET mechanism.[147] A doped molecular templated polymer was obtained by electropolymerization. The fluorescence signal from the sensor was amplified by the FRET process between the sensor and the doped molecularly imprinted polymer. This sensor was used to detect dimethoate in real samples with a good recovery (varying from 95% to 106%), and its LoD under ideal conditions was 1.83×10^{-11} mol L^{-1}.

Phosphoramidates. It has been demonstrated that phosphoramidates can control the growth of distinct varieties

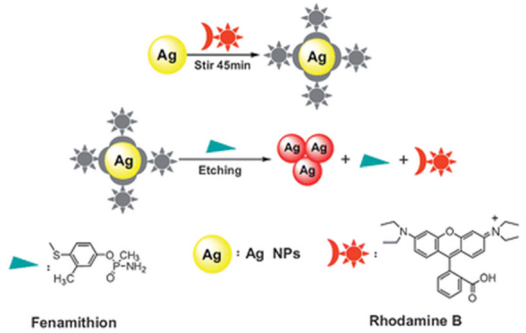

Fig. 9 The proposed representation of fenamithion sensing based on RB-Ag NPs. Reprinted with permission from ref. 148. Copyright 2011 Royal Society of Chemistry.

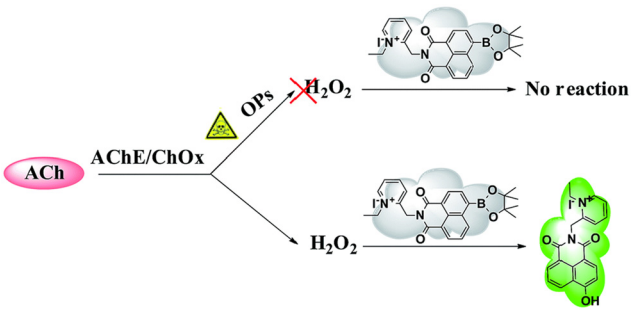

Fig. 10 The proposed sensing strategy to detect organophosphorus pesticides using boronate-1,8-naphthalimide fluorescent dye. Reprinted with permission from ref. 149. Copyright 2016 Royal Society of Chemistry.

of nematodes. Cui *et al.* developed a rhodamine B (RB) modified silver nanoparticles (RB-Ag NPs) based fluorescent and colorimetric probe to detect fenamithion in an aqueous solution with a better LoD of 10.000 nM (see Fig. 9).[148] Additionally, the sensor can be utilized to know the presence of fenamithion in real veggies and other water samples.

Phosphoramidothioate. In 2016, Shen *et al.* developed a new water-soluble fluorescent probe made from 1,8-naphthalimide dye and quaternary ammonium salt along with a boronate group to detect organophosphates such as trichlorfon, methyl parathion, and acephate (Fig. 10).[149] The probe displayed some advantages like high sensitivity, rapid colorimetric and fluorescence responses towards pesticides, and also the LoD for trichlorfon, methyl parathion, and acephate was 4.72×10^{-9} g L^{-1}, 3.36×10^{-10} g L^{-1}, and 1.16×10^{-9} g L^{-1}, respectively. In addition, the probe can detect pesticides in real samples with good results. The detection of omethoate and isocarbophos pesticides was accomplished by Dou *et al.* in 2015 by the utilization of a fluorescent approach that was based on a nanobeacon probe made of gold.[138]

Nitrophosphates. In 2021, Bai *et al.* reported a MOF-based fluorescent sensor Co-MOF made from 2-amino-terephthalic *via* a mixed solvothermal route and employed it to detect OPPs having *p*-nitrophenyl groups such as bis(*p*-nitrophenyl) phosphate (BNPP) and nitrophenyl phosphate (PNPP). The sensor's initial strong fluorescent emission was quenched in the presence of OPPs.[150] This method can be applied for OPP detection in various matrixes like water, food, and fruits. The detection limit was found to be 352 nM.

Phosphorothioates. Sun *et al.* developed highly fluorescent nanostructures from the reaction of molecularly imprinted polymers (MIPs) with silica particles which contained embedded CdSe nanospheres to detect parathion methyl.[151] Due to proximity-induced fluorescence quenching, the fluorescence intensity was significantly reduced when parathion methyl bound to the MIP. Notably, the sensor may be used to identify methyl parathion in plants. By combining gold nanoparticles (energy acceptors) with up-conversion nanoparticles (UCNPs) of europium and ytterbium (energy donors), Long *et al.* created a nanosensor that uses fluorescence resonance energy transfer to detect different organophosphorus, including parathion-methyl, monocrotophos, and dimethoate (Fig. 11).[152] The detection limits were determined to be 0.67, 23, and 67 ng L^{-1}, respectively. The detection mechanism was based on the fluorescence quenching of UCNPs by gold nanoparticles (AuNPs) and inhibition of AChE activity by organophosphorus pesticides.

Using fluorescence quenching as a basis, Tang *et al.* synthesized molecularly imprinted CdTe nanoparticles with molecular recognition ability for organophosphorus detection.[153] When compared to diazinon, chlorpyrifos, and pyrimithate, the synthesized compound exhibited a notable selectivity and strong binding affinity towards parathion, allowing for high recoveries (97.72% to 100.59%) of parathion detection in water samples. In 2017, the Song group developed an N-doped carbon dots (NCD) fluorescent probe for analyzing methyl parathion, and the LoD was found to be 0.338 μmol L^{-1}.[154] Of note, the present method was applied to detect methyl parathion in agricultural and real-world samples. Yan and team created a fluorescent probe based on $CuInS_2$-QDs and Pb(II) for methyl parathion detection.[155] Using nitrogen-containing heterocyclic 1,10-phenanthroline and 4-hydroxybenzylidene imidazolinone, Hu and colleagues produced Eu(III) complexes that showed fluorescence emission due to energy transfer. When methyl

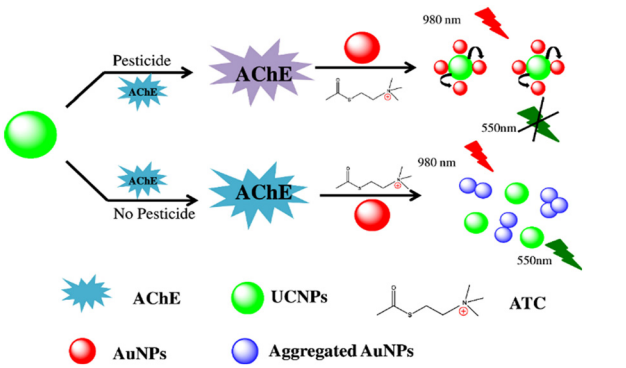

Fig. 11 Schematic representation of the UCNPs-AuNPs fluorescence assay for the detection of pesticides. Reprinted with permission from ref. 152. Copyright 2015 Elsevier.

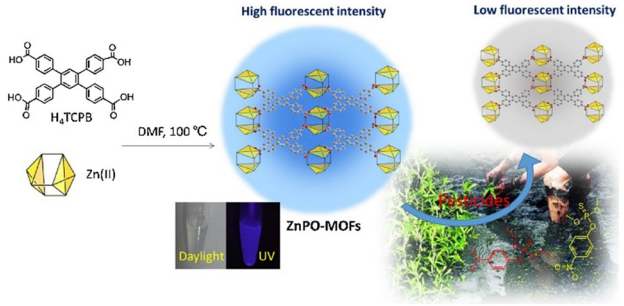

Fig. 12 Schematic representation for the synthesis of ZnPO-MOF and its application in organophosphorus detection. The strong blue emission of ZnPO-MOF was quenched in the presence of pesticides. Reprinted with permission from ref. 157. Copyright 2018 Elsevier.

parathion was added, fluorescence quenching occurred at λ = 617 nm, and a LoD of 95 nM was noted.[156]

To monitor methyl parathion, Xu *et al.* created a highly luminous ZnPO-MOF with 1,2,4,5-tetrakis(4-carboxyphenyl) benzene as a luminescent chemosensor.[157] ZnPO-MOF exhibited high selectivity for methyl parathion through a fluorescence turn-off mechanism (Fig. 12). The probe could detect methyl parathion at as low as 0.456 nM concentrations. This method can be applied to parathion-methyl detection in irrigation water. He and his team developed a water-stable luminescent zirconium MOF (Zr-MOF) from the reaction of Zr(IV) and 1,2,4,5-tetrakis(4-carboxyphenyl)benzene for the detection of methyl parathion in spiked food and environmental samples with low LoD values.[158] In another example, Eu(III) complexes containing amino-substituted β-cyclodextrin detect the presence of fenitrothion and the detection limit was as low as 1×10^{-12} M. The observed result was due to the encapsulation of fenitrothion in the inside cavity of the per-6-amino-β-cyclodextrin:Eu(III) complex which is the consequence of the absorption energy transfer emission (AETE) process.[159]

Using a time-resolved approach, Azab *et al.* developed a new fluorescence sensor called europium-allyl-3-carboxycoumarin (Eu(III)-ACC) to detect endosulfan, crotoxphos, and chlorpyrifos in water.[160] The probe was fluorescent but the fluorescence of the probe was quenched in the presence of chlorpyrifos and crotoxphos whereas the presence of endosulfan in the target sample increased the fluorescence of the probe. The LoD was observed to be 6.53 μmol L^{-1} for chlorpyrifos, 3.72 μmol L^{-1} for crotoxphos, and 0.004 μmol L^{-1} for endosulfan. They have prepared europium-doped titanium oxide nanopowder by the sol–gel method and used it to detect chlorpyrifos with significant fluorescence quenching.[161] The existence of an electron transport mechanism was discovered through experimental and computational investigations. To detect the insecticide chlorpyrifos (CPF), Ren's team created a fluorescent probe, such as Mn(II)-doped ZnS quantum dots coated with an acrylamide-based molecularly imprinted polymer (MIP-coated QDs). The LoD was determined to be 17 nmol L^{-1}. Chlorpyrifos could be found in actual samples using this simple, safe, and affordable approach.[162]

The development of a plant-based carbon dot fluorescence sensor has been reported by Tafreshi *et al.* for the qualitative and quantitative analysis of pesticides (diazinon, glyphosate, and amicarbazone) in water and in plant nutritional products.[163] The LoD was found to be 0.25, 0.5, and 2 ng ml^{-1} for diazinon, amicarbazone, and glyphosate, respectively, and the developed sensor can be applied for the detection of pesticides in real-world samples. In 2019, Arvand *et al.* reported an efficient fluorescent sensor based on L-cysteine capped CdS-QDs/DF20 to analyze diazinon in environmental and agriculture samples based on the FRET mechanism, and the LoD was found to be 0.13 nM (Fig. 13).[164] Ibrahim and coworkers synthesized a fluorescent probe, Tb(III) complex of 3-ally-salicylohydrazide, for detecting dichlorvos.[165] The probe possessed good luminescence properties and the fluorescence at λ = 546 nm was enhanced with the addition of dichlorvos. Lu *et al.* have synthesized a Hg(II) complex of novel cholesterol derivative, 4-chloro-7-nitro-1,2,3-benzoxadiazole (CTN) using triazole as a linker, that showed a fluorescent emission at λ = 561 nm.[166] The sensor detected five major organophosphorus pesticides, glyphosate, dichlorvos, chlorpyrifos, diazinon, and phoxim, with detection limits of 0.015, 0.018, 0.087, 0.098, and 0.113 μg mL^{-1} and the intensity of fluorescence emission gradually raised with the blue shift from λ = 561 to 527 nm in the presence of any of these pesticides. Kaur *et al.* developed two distinct Biginelli derivatives of cobalt complexes to enable the detection of malathion and azamethiphos using the fluorescence turn-on method. The LoD values for malathion and azamethiphos were 9.2 nM and 11 nM in aqueous medium, respectively.[167]

Phosphonates. In 2021, Guan *et al.* synthesized a small organic molecule fluorescent rhodamine derivative, which specifically detected glyphosate based on the Cu(II)-indicator displacement strategy.[168] This technique involves the displacement of an indicator (R–G) from a Cu(II)-indicator complex by glyphosate. This displacement occurs because glyphosate has a high affinity for interacting with Cu(II),

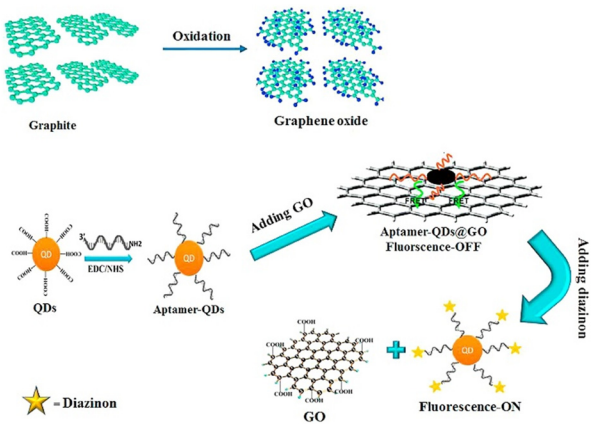

Fig. 13 The principle of the fluorescence "turn off–on" aptasensor for diazinon detection based on QDs-aptamer and GO. Reprinted with permission from ref. 164. Copyright 2019 Elsevier.

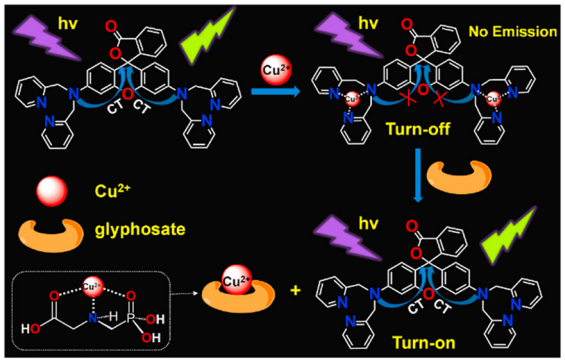

Fig. 14 Schematic illustration of glyphosate sensing based on the Cu(II)-indicator displacement strategy. Reprinted with permission from ref. 168. Copyright 2021 Elsevier.

which results in fluorescence activation. The LoD for glyphosate was observed to be 4.1 nM, and this method detected glyphosate in the surface of cabbage and spiked soil samples (Fig. 14). As an illustration, *p-tert*-butylcalix[4]arene was bound to silicon nanoparticles containing ruthenium. A detection limit of 7.91×10^{-7} M was established when glyphosate was detected using this method and the FRET process.[169] Another example of the use of carbon quantum dots was given by Hou *et al.*, where fluorescence quenchers—more especially, Fe(III) cations—were used. Strong interactions between the glyphosate and the Fe(III) cations caused the cations to be removed from the area around the carbon dots, restoring the fluorescence. Experimental studies showed that the fluorescence between the carbon dots and Fe(III) cations was extinguished by electron transfer.[170] The Wang group reported a fluorescence system made up of CDs with AgNPs (CDs/AgNPs) for the detection of glyphosate. The CDs/AgNPs system exhibited a direct proportionality to the glyphosate concentration (0.025–2.5 μg mL^{-1}) under optimized conditions. The detection limit was set at 12 ng mL^{-1}. In addition, cereal samples containing glyphosate have been detected using this technique with favorable outcomes.[171]

Yang *et al.* prepared a metal–organic framework-based novel sensor Zr-MOF, Fe_3O_4@SiO_2@UiO-67 *via* a versatile layer-by-layer assembly strategy for the detection of glyphosate.[172] The fluorescence was enhanced due to the interaction of Zr-MOF with glyphosate and the LoD was 0.093 μg L^{-1}. Guo *et al.* designed a turn-on fluorescence probe for the detection of glyphosate, based on the FRET mechanism between CdTe QDs capped with thioglycolic acid (TGA-CdTe-QDs) and gold nanoparticles stabilized with cysteamine (CS-AuNPs). This technique has been applied to successfully and satisfactorily identify glyphosate in apples and the LoD was found to be 9.8 ng kg^{-1}.[173] Yu *et al.* developed a sensor by combining two supramolecular systems such as two-dimensional MOF nanosheets with calix[4]arenes for glyphosate detection. A substantial increase in fluorescence emission was observed in the presence of pesticides based on electron transfer.[174] The fluorescence sensing properties of various sensors highlighted in this article for organophosphate pesticide detection are given in Table 2.

4.2 Fluorescence sensing of carbamate pesticides

Carbamates are the derivatives of carbamic acid with ester and thioester functionalities.[178] They are comparably safer to use than organophosphates, organochlorines, and pyrethroid pesticides.[179] Despite having low bioaccumulation, they have been found to disrupt endocrine.[180] Acetylcholinesterase enzyme required for the hydrolysis of acetylcholine is the main target of these compounds, where they induce carbamylation at neuromuscular junctions and neuronal synapses and inhibit acetylcholine breakdown.[179–181] Few carbamates have been commercialized as drugs like rivastigmine (for treating Alzheimer's and Parkinson's disease), urethane (for chemotherapy), meprobamate (for anxiety), darunavir (an antiretroviral drug) and carbachol (for ophthalmic irregularities).[182] Nevertheless, they are majorly applied as pesticides in agriculture and their maximum residue limit (MRL) can vary between 0.01 and 100 mg kg^{-1}.[178–183] Remaining levels of oxamyl, carbofuran, aldicarb, methomyl, benomyl, methiocarb, carbendazim, and pirimicarb have been detected in agricultural goods.[178,180,181] Monitoring environmental samples for carbamate pollutants has become crucial due to the effects that prolonged use of carbamates has had on non-target organisms.[184–186] Common carbamate pesticides are highlighted in Fig. 15.

The application of colorimetric and fluorescence methods for carbamate detection has been the subject of several reports. The probes used range from basic organic molecules to quantum dots and nanoparticles. The majority of fluorescent probes for carbaryl detection that have been reported were chosen based on how well they worked with the enzyme carboxylesterase, which has an ester group. Under experimental conditions, the probe works by hydrolyzing the ester into acid (see Fig. 16). When there is an

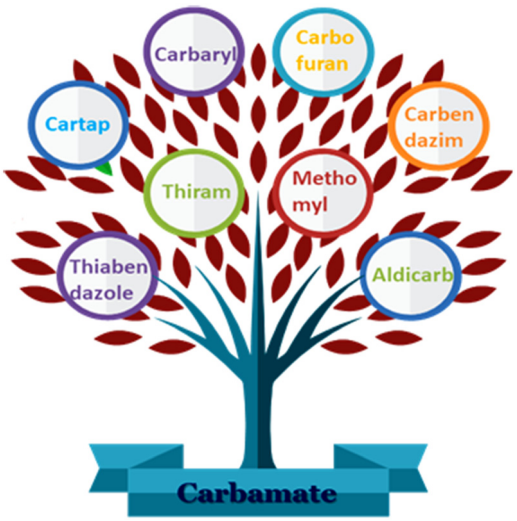

Fig. 15 Examples of carbamate pesticides.

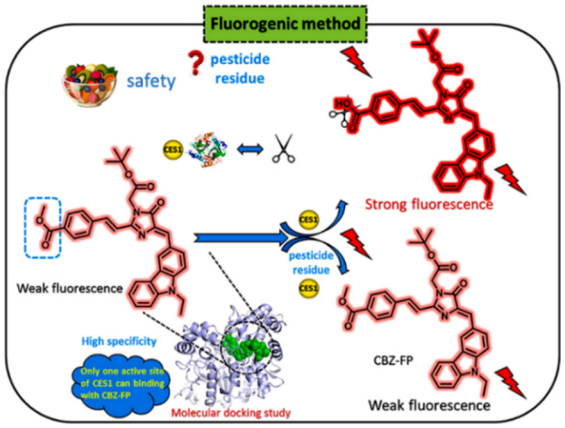

Fig. 16 The mechanism of fluorescence off–on sensing of carboxylesterase and carbaryl pesticide. Reprinted with permission from ref. 187. Copyright 2021 Elsevier.

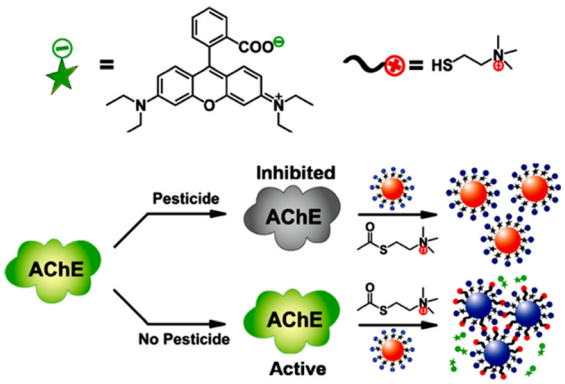

Fig. 17 The schematic illustration of the design of dual mode of colorimetric and fluorometric assays for the detection of pesticides. Reprinted with permission from ref. 189. Copyright 2012 American Chemical Society.

increase in the quantity of carbaryl, the carboxylesterase inhibition activity is enhanced, thereby the emission of the probe gets suppressed.[187,188] Carbaryl detection has been accomplished by nanoparticles as probes, in which the inhibition of acetylcholinesterase activity was applied as a strategy. For instance, a rhodamine B-covered gold nanoparticle with a dual method of detection (fluorescence and colorimetric) reported by Liu *et al.* (see Fig. 17)[189] and carbon quantum dots coupled with nanoparticles reported by Chen *et al.* demonstrated substantial quenching of the fluorescence intensity upon the addition of carbaryl pesticide.[190,191]

A colorimetric sensor array has been fabricated with five hydrogen peroxide and thiocholine-sensitive probes for carbamate detection (carbaryl, metolcarb, methomyl, isoprocarb, fenobucarb). The prevention of thiocholine production has been used as a base for this detection.[192,193] Cadmium telluride (CdTe) quantum dots have been formulated as sensors for the detection of carbaryl in rice, Chinese cabbage (LoD = 0.147 μM), and Iranian apple (see

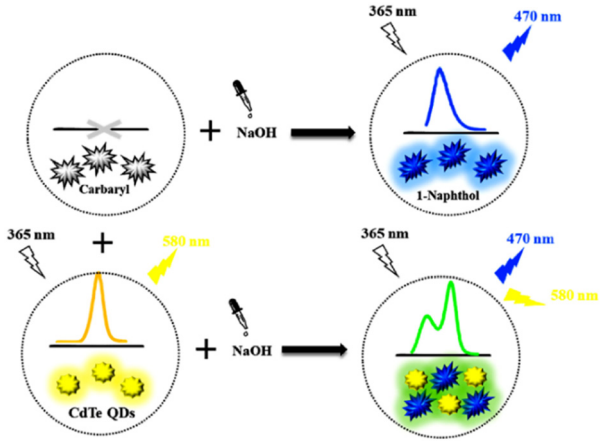

Fig. 18 The proposed ratiometric fluorescence nanoprobe using CdTe QDs for the detection of carbaryl pesticide. Reprinted with permission from ref. 194. Copyright 2021 Elsevier.

Fig. 18).[194] Carbendazim, because of the presence of benzimidazole, possesses significant chemical stability and exists for a longer period in the environment. Cucurbits have been used for this purpose, which mainly function by complex formation with carbendazim. This newly formed interaction enhanced the fluorescence intensity of the pesticide residue and allowed its detection even with low concentrations.[195,196]

Yang *et al.* have demonstrated the detection of carbendazim (with a LoD of 0.002 μM) using a combined probe established from N,P-doped carbon quantum dots and AuNPs based on the FRET mechanism (Fig. 19).[197] Similarly, S-doped graphene QDs were used as sensors for the detection of carbofuran and thiram with a LoD of 0.45 ppb and 1.6 ppb, respectively (Fig. 20),[198] and vitamin B_{12} coated carbon QDs with dual fluorescence emission for detecting carbofuran were developed, which involves the charge transfer complex formation by carbofuran on the surface of QDs.[109]

Core–shell QDs have been used to selectively detect trace levels of carbamate insecticides (carbofuran, aldicarb, and methomyl) found in medicinal plants. Acetylcholinesterase was

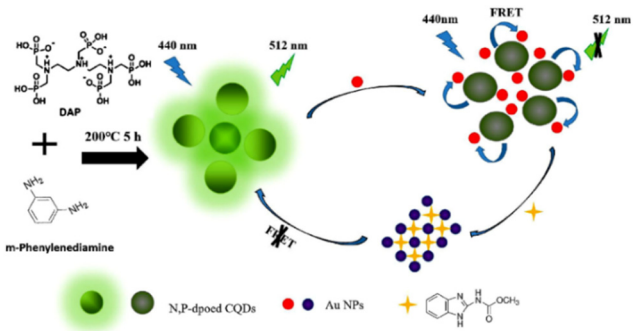

Fig. 19 The formation of N,P-doped carbon quantum dots and their use to detect carbendazim pesticide *via* the FRET mechanism. Reprinted with permission from ref. 197. Copyright 2018 Elsevier.

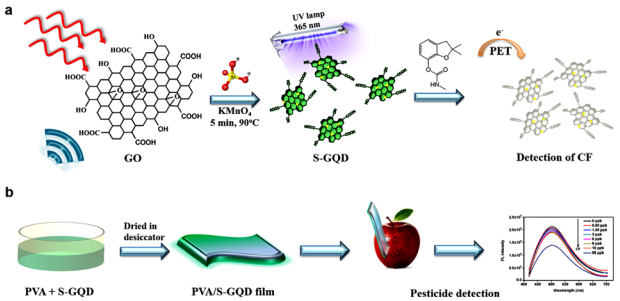

Fig. 20 (a) The microwave-assisted sonochemical synthesis of S-GQD, and (b) the fabrication of S-GQD-based fluorescent (PVA/S-GQD) films for the sensitive detection of carbofuran. Reprinted with permission from ref. 198. Copyright 2020 Elsevier.

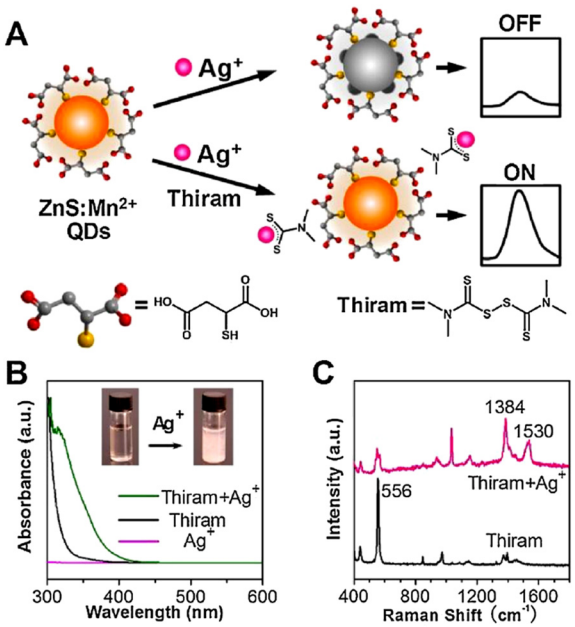

Fig. 21 (A) The sensing mechanism for the detection of thiram. (B) UV-vis absorption spectra of Ag(I), thiram, and Ag–thiram complex (inset: colloidal suspension of the complex). (C) The Raman spectra of thiram and Ag–thiram complex. Reprinted with permission from ref. 200. Copyright 2017 Elsevier.

effectively inhibited by carbamates in this fluorescent sensing method. Carbofuran had the strongest inhibitory activity among the carbamates that were evaluated.[199] Zhang *et al.* have developed a "turn-on" sensor for thiram by using Mn-doped ZnS QDs combined with Ag(I) ion. Inhibition of the quenching process takes place due to the formation of a stable thiram–Ag(I) complex (Fig. 21) with a LoD of 25 nM in fresh fruits.[200] Recently, a fluorescent probe based on multi-color nitrogen dots for sensing thiram and chlorpyrifos in pear, lettuce, lychee, orange, and cucumber samples was reported by Tang *et al.*, in combination with copper and iron ions.[201]

A sensitive and selective fluorescent probe has been constructed from an MOF functionalized with Zr(IV) and Tb(III) for detecting thiabendazole in oranges. This system can sense thiabendazole in about 35 minutes, with a LoD of 0.271 μM. This is because energy transferred from the MOF to thiabendazole causes the fluorescence intensity to be quenched.[202] The complex formation of thiabendazole with cucurbit[6]uril and cucurbit[7]uril, and cartap with cucurbit[7]uril has been formulated as a strategy for their detection. When the complexation was initiated, the fluorescence of thiabendazole became enhanced in neutral aqueous medium with a detection limit in the range of 5.51 to 8.85 × 10^{-9} mol L^{-1},[203] and quenching in the case of cartap with a LoD of 0.0029 μg mL^{-1}.[204] A hybrid chemosensor developed from $NaYF_4$:Yb, Ho/Au nanocomposites has been used for the detection of cartap in farm and water samples. The presence of cartap caused aggregation of nanocomposites, which in turn enhanced the FRET process between $NaYF_4$:Yb, Ho, and Au nanocomposites.[205] Zeng *et al.* reported the detection of metolcarb by using a naphthol appended calix[4]arene (NOC4) combined with a micro-structured gold surface. Because of the new complex formation, the fluorescent emission was found to be enhanced with a detection limit of 0.1 μM.[206] It was reported that the initial fluorescence intensity of rhodamine B functionalized AuNPs was restored in the presence of thiodicarb.[207]

Disruption of aggregation produced by pyrene appended β-cyclodextrin in aqueous solution was observed by the introduction of pirimicarb. The same probe was employed for the detection of common aromatic trinitro explosives like trinitrotoluene, picric acid, and trinitrobenzene.[116] Highly luminescent CdTe QDs coated with 5,11,17,23-tetra-tert-butyl-25,27-diethoxy-26,28 dihydroxycalix[4]arene (C[4]/SiO_2/CdTe) allowed the sensitive detection of methomyl *via* significant enhancement in fluorescence, which exhibited a linear relationship with methomyl concentration and showed a LoD of 0.08 μM (Fig. 23).[208] It has been reported that cyclodextrins can be used for fluorescence-based herbicide detection, in which binding to cyclodextrin increases the emission intensity of weakly fluorescent carbamate pesticides.[209,210] In

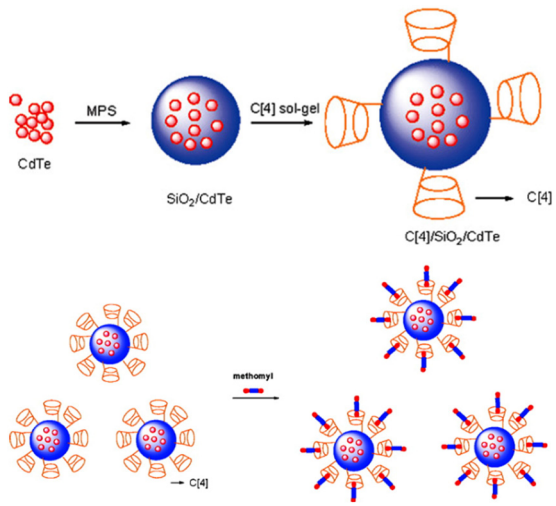

Fig. 22 The fabrication of the C[4]/SiO_2/CdTe luminescent probe and its pesticide sensing through host–guest complexation. Reprinted with permission from ref. 208. Copyright 2007 American Chemical Society.

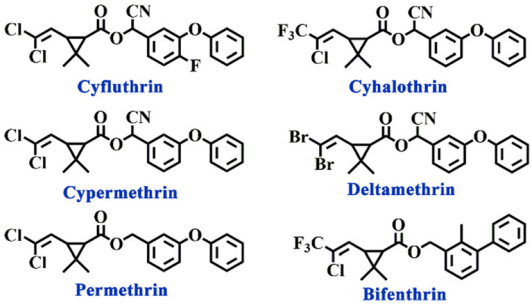

Fig. 23 Some common pyrethroid pesticide derivatives.

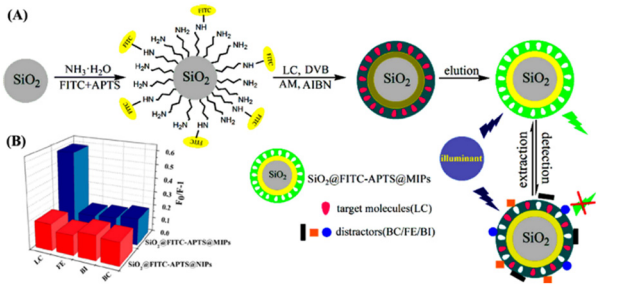

Fig. 24 (A) Schematic illustration of the synthesis of SiO_2@FITC-APTS@MIPs fluorescence sensor and (B) the extent of fluorescence quenching by different kinds of pyrethroid pesticides. Reprinted with permission from ref. 218. Copyright 2015 American Chemical Society.

the presence of either β- or γ-cyclodextrin, bendiocarb and promecarb showed 1.74 and 3.8-fold increases in fluorescence emission, respectively (Fig. 22).

A turn-off fluorescence sensor for the identification and detection of cartap and methyl thiophanate has been published by Fan *et al.* This work involved the approach of simultaneously using water-soluble cadmium QDs (ZnCdSe and CdSe QDs) for the detection of the analyte. In real-time samples, the LoD was found to be 2×10^{-8} mol L^{-1}.[211] Table 3 summarizes the sensing properties of various fluorescence probes discussed in this article for selective detection of carbamates.

4.3 Fluorescence sensing of pyrethroid pesticides

Pyrethroids are a class of pesticides derived from pyrethrins, which are commonly used as insecticides. They are moderately toxic and possess moderate biodegradability. Nearly 70 pyrethroid derivatives have now been applied in agriculture, and some of their structures have been shown in Fig. 24.[212] However, because of their high absorbability, they have an impact on animal development and raise the risk of cancer with extended exposure. Pyrethroids can sometimes be detrimental to plant growth.[213–215] and it has been suggested that sperm count is affected in post-pyrethroid exposure.[216,217] There are only limited reports available for the identification and detection of pyrethroids, which include sensors, surface-enhanced Raman scattering, and surface plasmon resonance.

Fluorescent MIPs have been identified as a method for pyrethroid detection. MIP microspheres are made by precipitation polymerization with allyl fluorescein as a monomer and the cyhalothrin analyte as a template. This template was utilized to identify the analyte in actual honey samples and demonstrated great sensitivity and selectivity for cyhalothrin.[219] Another report was made by Liu and co-

Table 3 Summary of fluorescence sensing properties of various sensors for carbamate pesticide detection (other class analytes are mentioned to highlight the selectivity of sensors)

Probe	Analyte	LOD	Ref.
Rhodamine B covered gold nanoparticles	Carbaryl, diazinon, malathion, phorate	Carbaryl 0.1 μg L^{-1}, diazinon 0.1 μg L^{-1}, malathion 0.3 μg L^{-1}, phorate 1 μg L^{-1}	189
CdTe QDs	Carbaryl	0.147 μM	193
CdTe QDs	Carbaryl	0.12 ng mL^{-1}	194
Cucurbit[7]uril	Carbendazim	0.10 mg kg^{-1}	196
N,P-doped carbon quantum dots and AuNPs	Carbendazim	0.002 μM	197
S-doped graphene QD	Carbofuran	0.45 ppb	198
	Thiram	1.6 ppb	
Vitamin B_{12} coated carbon QD	Carbofuran	12.2 μM	109
Mn-doped ZnS QD- Ag^+ ion	Thiram	25 nM	200
Nitrogen dots combined with copper and iron ions	Thiram	0.1 μg mL^{-1}	201
	Chlorpyrifos	0.01–0.50 μg mL^{-1}	
Tb^{3+} functionalized Zr-MOF	Thiabendazole	0.271 μM	202
Cucurbituril	Thiabendazole, cartap	5.51–8.85 × 10^{-9} mol L^{-1}	203
		0.0029 μg mL^{-1}	204
$NaYF_4$:Yb, Ho/Au nanocomposites	Cartap	0.0029 μg m L^{-1}	205
Naphthol appended calix[4]arene@gold surface	Metolcarb	0.1 μM	206
Rhodamine B functionalized Au NPs	Thiodicarb	0.08 ppm	207
β-Cyclodextrin	Pirimicarb	60 nM	116
C[4]/SiO_2/CdTe	Methomyl	0.08 μM	208
Cyclodextrin	Bendiocarb	0.57 ± 0.02 μg mL^{-1}	209, 210
	Promecarb	0.091 ± 0.002 μg mL^{-1}	
ZnCdSe-CdSe QD	Methyl thiophanate	2 × 10^{-8} mol L^{-1}	211

workers, who developed supramolecular architectures containing an MIP based on a luminescent Eu complex and Si nanospheres. The resultant template used analyte-induced fluorescence quenching to detect λ-cyhalothrin with great selectivity.[220] To create a composite pesticide sensor, Wei *et al.* combined luminescent CdTe quantum dots with MIPs synthesized in the presence of a bifenthrin template. This resulted in a marked decrease in fluorescence emission due to bifenthrin binding, with very low detection limits and high levels of selectivity reported. The synthetic method induces polymerization on the CdTe quantum dot surfaces using a biphasic solvent solution.[221] Silica-based MIPs have been used for detecting cyhalothrin with the help of silica nanospheres embedded in CdSe QDs and SiO_2.[218,222,223] These methods eliminated the interfering materials in the sample and improved the LoD value (see Fig. 24).

Wei *et al.* created a fluorescent technique to detect λ-cyhalothrin by transferring aqueous CdTe QDs using octadecyl-4-vinylbenzyl-dimethyl-ammonium chloride (OVDAC) as a surfactant (Fig. 25).[224] The Ren team created MIPs and employed them to produce a composite material coated with MIPs, using QDs. This composite material was designed to selectively recognize cyphenothrin.[225] A new, eco-friendly MIP-QD nanosensor has been developed to specifically extinguish cyfluthrin's fluorescence. This nanosensor was created using an enhanced reverse microemulsion process and is based on FeSe-QDs. The ionic and hydrogen bonding interactions prevented charge transfer from FeSe-QDs to cyfluthrin and produced excellent linearity, selectivity, and sensitivity.[226]

A fluorescent MIP sensor was developed specifically for detecting pyrethroid pesticides by using SiO_2/ZnO QDs. This sensor has a very low (LoD) of 0.13 μM. The sensor demonstrated a quick and selective detection of cyhalothrin in practical river-water samples within a 15-minute

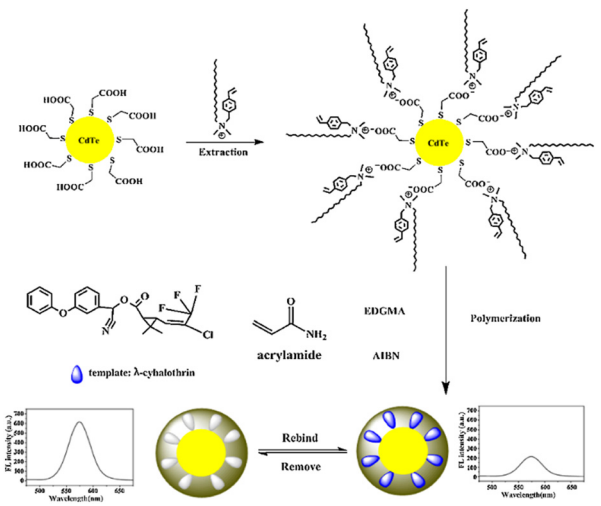

Fig. 25 Schematic illustration for the preparation of MIPs-OVDAC/CdTe QDs and their fluorescence-quenching-based sensing of λ-cyhalothrin antibiotics. Reprinted with permission from ref. 224. Copyright 2016 Elsevier.

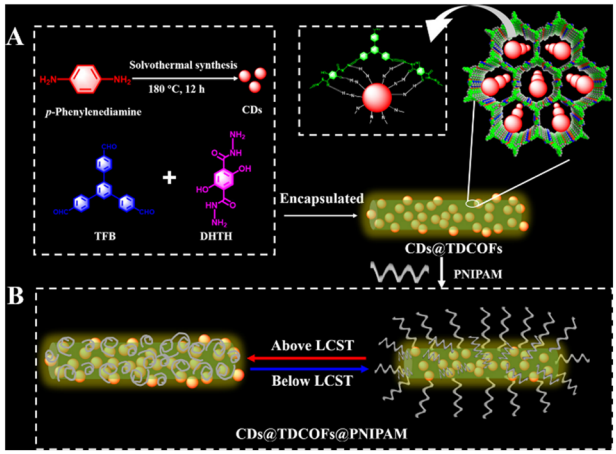

Fig. 26 Schematic representation of (A) the fabrication of the CDs@TDCOFs@PNIPAM fluorescence sensor for (B) on/off detection of pyrethroids. Reprinted with permission from ref. 229. Copyright 2022 American Chemical Society.

timeframe.[227] Atom transfer radical polymerization has been used to construct a sensor composed of a MIP.[228] Cyhalothrin can be detected using this sensor. Within the range of 2–80 nM, the fluorescence intensity of SiO_2-MPS@FMIP, which is composed of a fluorescent MIP and a SiO_2 core modified with MPS (3-(methacryloxyl) propyl trimethoxysilane), showed a linear relationship with the cyhalothrin concentration. Cyhalothrin's LoD was found to be 0.0037 nM.[229]

Using CD functionalized core–shell nanospheres, dual emission determination of λ-cyhalothrin has been established by tracking the transition from green to blue fluorescence.[230] Sulfur-doped carbon dots coated with MIPs utilizing acrylamide and 1-vinyl-3-butylimidazolium tetrafluoroborate [VBIm][BF_4] were used to detect LC, a pesticide residue that shows a LoD of 0.5 μg kg^{-1}.[231] A ZnO-based MIP containing cyhalothrin recognition sites exhibited a linear relationship between the concentration of cyhalothrin and the fluorescence intensity obtained in the concentration range of 0 to 80 μmol L^{-1}.[232] To identify deltamethrin in fruit and vegetable samples, water-soluble CdTe QDs and fluorescent SiO_2 molecularly imprinted nanospheres embedded in CdTe QDs functioned as a fluorescence nanosensor.[233] CD-encapsulated covalent organic frameworks grafted with poly(*N*-isopropyl acrylamide) were developed for the detection of pyrethroids, which are temperature-responsive and have a detection limit of 0.69 μg L^{-1} (Fig. 26).[229] Two molecularly imprinted polymeric microspheres and two fluorescent tracers for benzimidazoles and pyrethroids were fabricated and used for the simultaneous determination of benzimidazoles and pyrethroids with a LoD ranging from 5.2 to 17 ng mL^{-1}.[234]

A novel host–guest supramolecular probe with an albumin host and flavonoid guest was successfully synthesized for the ratiometric determination of cyfluthrin with a fast detection response of 10 s and a LoD of 70 ppb along with a distinct orange to green emissive color change. The smartphone-

Table 4 Summary of fluorescence sensing properties of various sensors for pyrethroid pesticide detection

Probe	Analyte	LoD	Ref.
Molecularly imprinted polymers microspheres	Cyhalothrin	0.004 nm	219
m-SiO_2-Eu(TTA)$_3$Bpc@MIPs	λ-Cyhalothrin		220
MIPs (PS)-OVDAC/CdTe QDs	Bifenthrin	0.08 μmol L^{-1}	221
CdSe QDs-SiO_2-MIPs	λ-Cyhalothrin	3.6 μg L^{-1}	222
Molecularly imprinted fluorescent hollow nanoparticles	λ-Cyhalothrin	10.26 nM	223
SiO2@FITC-APTS@MIPs	λ-Cyhalothrin	9.17 nM L^{-1}	218
MIPs-octadecyl-4-vinylbenzyl-dimethyl-ammonium chloride (OVDAC)-CdTeQDs	λ-Cyhalothrin	0.03 μmol L^{-1}	224
QDs-based MIPs-coated composite (ZnS-Mn^{2+})	Cyphenothrin	9.0 nmol L^{-1}	225
MIP-FeSe-QDs	Cyfluthrin in fish	1.0 μg kg^{-1}	226
SiO_2-MPS@FMIP	Cyhalothrin	0.0037 nM	228
CDs-SiO_2	λ-Cyhalothrin	0.048 μg L^{-1}	230
Sulfur-doped carbon dots - MIPs	λ-Cyhalothrin	0.5 μg kg^{-1}	231
SiO_2-MIPs-CdTe QDs	Deltamethrin	0.16 μg ml^{-1}	233
Host–guest supramolecular probe with an albumin host and flavonoid guest	Cyfluthrin	70 ppb	235
Boron-based non-covalent ratiometric fluorophore	Pyrethroids	1.5 μg L^{-1}	236

assisted on-site analysis enabled the signal outputs to be captured and analyzed.[235] A fluorophore synthesized from the interaction between two boron derivatives with the nickel complex as a catalyst and triphenylphosphine as an additive exhibited a dual emissive phenomenon. The intensity ratio of these two emissions served as a ratiometric method for the detection of pyrethroids and recorded a LoD of 1.5 μg L^{-1}.[236] Table 4 summarizes the selective detection of pyrethroids using fluorescent probes.

4.4 Fluorescence sensing of triazine and triazole pesticides

Triazine and triazole moieties find widespread use as pesticides in crop production like sugar cane, grapes, corn, rice, and pulses. Their water solubility enables them to stay in the soil for a long time, and this stability may have ill effects on water and food.[237] HPLC, GC, MS, and GC-MS were among the methods utilized to identify and quantify their contamination. However, since these techniques fail to identify traces of remaining pesticides, an effective detection technique needs to be created.[238,239] Examples of triazine and triazole pesticides are given in Fig. 27 and 29.

Triazines. Wang *et al.* created two single template MIPs and a dual template MIP to detect 14 herbicides at once.[240] Prometryn and atrazine were chosen as the templates, and the extraction procedure was facilitated by the structural similarities between the template molecules from maize samples and herbicides and their metabolites. Of note, dual-templates were superior to multiple single-templates in terms of analyte affinities and recoveries. In 2021, Zoughi *et al.* employed an optical nanosensor fabricated with a carbon dot fluorophore for tartrazine detection through fluorescence quenching. Using this sensor, analysis was also carried out in ice cream, fake saffron, and saffron tea, producing a very low LoD of 1.3 nM.[241] Turn-on fluorescent probes including nitrogen-doped carbon quantum dots (N-CDs) were designed by Mohapatra *et al.* The fluorescence turn-on behaviour was observed when the probe interacted with atrazine by intermolecular hydrogen bonding. The detection limit was 3 μg

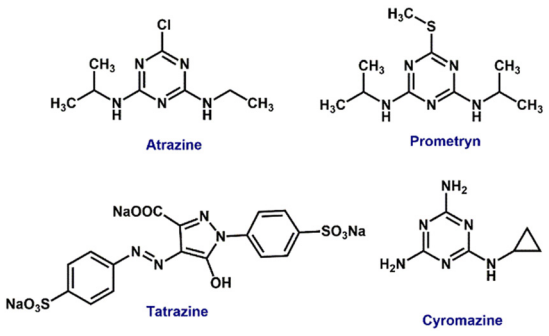

Fig. 27 Some common triazine pesticide derivatives.

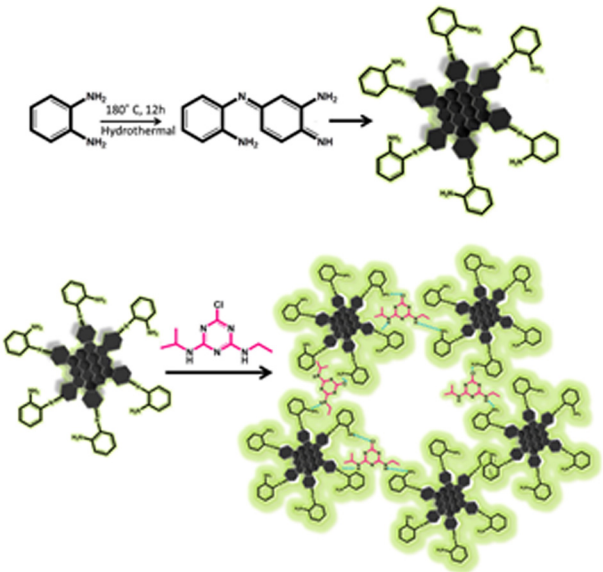

Fig. 28 The schematic representation of the synthesis of nitrogen-doped carbon quantum dots (above) and their turn-on fluorescent sensing of the herbicide atrazine through multiple hydrogen-bonding interactions (below). Reprinted with permission from ref. 242. Copyright 2018 Elsevier.

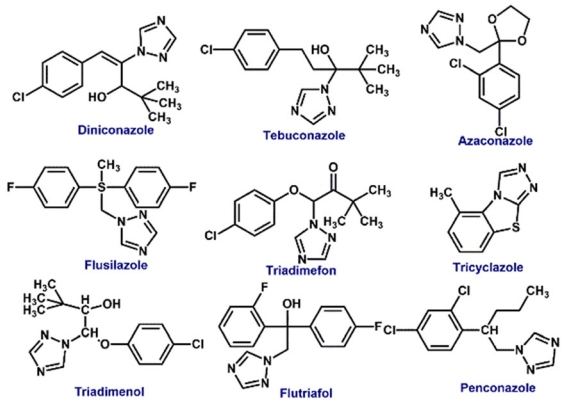

Fig. 29 Some triazole pesticide derivatives.

L^{-1} (Fig. 28). This sensor has been used on bacterial cells and actual samples.[242] Similarly, Sahoo *et al.* employed zinc oxide quantum dots as a fluorescence sensor to find atrazine.[243] Highly fluorescent CdSeTe/ZnS QDs were fabricated and encapsulated with MIPs for the selective detection of atrazine. The sensor response time for atrazine was fast (5 min) and the fluorescence intensity exhibited linear quenching within 2–20 mol L^{-1} of atrazine, with an LoD of 0.80×10^{-7} mol L^{-1}. The sensor also enabled detection in real water samples with about 92–118% recoveries.[244] In another study, Su *et al.* reported using gold nanoparticles for cyromazine sensing. The selective interaction between cyromazine and NP-containing gallic acid destabilized the nanoparticles by creating non-fluorescent aggregates, which reduced fluorescence emission intensity. Furthermore, there was a noticeable preference for cyromazine when contrasted with other pesticide analytes and other potential interfering anions and cations.[245]

Liu *et al.* developed a novel MIP-Fe_3O_4-chitosan-based sensor for the detection of atrazine and the method involved the direct competition between atrazine and its fluorescent analogue (5-(4,6-dichlorotriazinyl)amino fluorescein (5-DTAF)). Increased fluorescence was observed, with a LoD of 0.86 μM and a linear relationship with the log(atrazine) concentration in the range of 2.32 to 185.4 μM.[246] Halder and his colleagues conducted extensive computational research on luminous MOFs employed for pesticide detection. They examined a copper MOF and a cadmium MOF that both contained 4,4′-bipyridine ligands and succinate dianions as bridging components.[247] According to the study, succinate's oxygen atoms were necessary for coordinating with the NH and OH groups of the pesticides, particularly atrazine and dicofol. They also had aromatic π–π stacking between the bipyridine and aromatic pesticides. The second case involved the utilization of a magnetic covalent organic framework (COF) to identify chlorpyrifos, atrazine, and diquat dibromide in polluted water solutions.[248] The procedure entailed the pesticides adhering to the COF and then removing them using magnetic solid-phase extraction. Following the regeneration of the COF, this cycle was carried out up to five times.

Triazoles. In 2017, Amjadi and Jalili developed a dual-emission mesoporous structured MIP sensor encapsulated with CdTe/CdS QDs for the ratiometric detection of diniconazole (DNZ). In the concentration range of 20–160 μg L^{-1}, with a LoD of 6.4 μg L^{-1}, DNZ showed a linear correlation with DNZ and produced a visible green-to-blue color change by selectively quenching the ratiometric probe's fluorescence emission intensity (Fig. 30).[249]

To identify non-fluorescent triazoles such as azaconazole, flusilazole, tricyclazole, triadimefon, tebuconazole, penconazole, flutriafol, and triadimenol isomer A in aqueous solution, the host–guest complex of thioflavin T (ThT) and twisted cucurbit[14]uril (tQ[14]) was used as a fluorescent probe. Flusilazole caused a particular reaction in the ThT@tQ[14] probe, which led to a significant decrease in fluorescence intensity. The probe detected flusilazole at a minimum concentration of 1.27×10^{-8} mol L^{-1}.[250] In one example, researchers reported a thiazole-twisted cucurbit[14] uril (tQ [14]) (Li *et al.*, 2016), for fluorescence-based triazole-containing pesticide detection. Triazoles significantly reduced fluorescence when they were introduced. It was discovered that two distinct supramolecular mechanisms were at work: one in which the triazole and thiazole competed for the same binding site, ultimately leading to fluorescence quenching, and another in which the triazole bound to a different section of tQ [14] than thiazole, resulting in cooperative effects that facilitated the decreases in fluorescence intensity.[251]

4.5 Fluorescence sensing of organochlorine pesticides

Presently, the growing population necessitates the rapid production of vegetables, cereals, and fruits, resulting in the overutilization of pesticides, particularly organochlorine pesticides (OCPs) in crop agriculture and animal husbandry. Most of the OCPs are degraded slowly under standard environmental conditions. OCPs can enter the human body through the skin and lungs. They have the potential to impact the central nervous system, resulting in convulsions, hyperreflexia, ataxia, and tremors. Prolonged exposure to

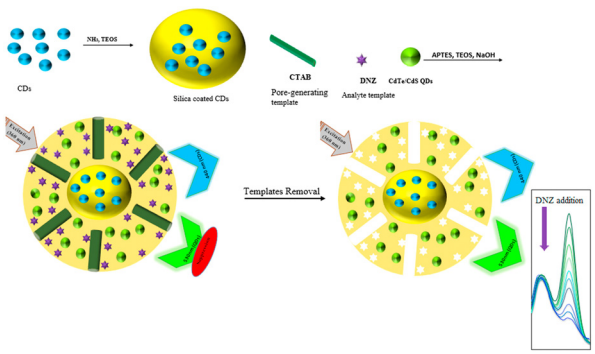

Fig. 30 The schematic representation of a dual-emission mesoporous structured MIP sensor encapsulated with CdTe/CdS QDs for the ratiometric detection of diniconazole. Reprinted with permission from ref. 249. Copyright 2017 Elsevier.

OCPs at low concentrations can lead to immunosuppression, reproductive abnormalities, hypersensitivity reactions, and potentially even cancer. Some of the organochlorine structures are given in Fig. 1. In this part of the review, the detection of organochlorines using fluorescence-based chemosensors has been discussed. Glutathione-coated CdS (GSH-CdS) QDs were reported by Walia and Acharya for the selective detection of dicofol, in the presence of other pesticides namely dimethoate, chlorpyrifos, and imidacloprid.[252] The chloride groups of dicofol interacted with the $-NH_2$ and –COOH groups of glutathione, increasing the fluorescence of GSH-CdS QDs to allow for "turn-on" detection, and the probe was able to detect dicofol down to 55 ± 11 ppb.

In another example, polar OCPs were detected using methylammonium lead halide perovskite QDs (MAPB-QDs) based on the observation that the fluorescence spectra of MAPB-QDs were blue-shifted when polar OCPs were present.[253] Wang *et al.* and Yang *et al.* have used Mn-doped ZnS QDs imprinted with an MIP for the detection of pentachlorophenol (PCP).[254,255] This probe can detect the spiked PCP in river water, tap water, and spring water with good recoveries. In another example, Liu *et al.* prepared the probe from the combination of graphene quantum dots GQDs with CdS QDs to form GQDs-CdS nanocrystals to detect the presence of pentachlorophenol in water samples.[256,257] To detect 2,4-dichlorophenoxyacetic acid (2,4-D), mesoporous structured imprinting microspheres were attached to quantum dots (QDs) to produce a novel fluorescence sensor.[258] An electron-transfer-induced fluorescence quenching process makes this detection possible. The sensor demonstrated a detection limit of 2.1 nM and was effectively utilized to detect 2,4-D in bean sprout samples. The recoveries achieved ranged from 95.0% to 110.1%, indicating great accuracy and precision.

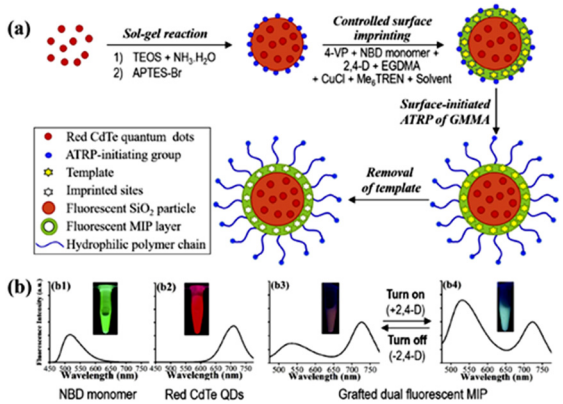

Fig. 31 (a) Fluorescence 'turn-on' optosensing of herbicide in pure milk using a ratiometric fluorescent microsphere. (b) Fluorescent spectra and fluorescence colors of the polymerizable NBD monomer (in CH_3CN, b1) and red CdTe QDs (in H_2O, b2) as well as those of the grafted dual fluorescent 2,4-D-MIP (b3) and its mixture with 2,4-D (b4) in pure bovine milk. Reprinted with permission from ref. 261. Copyright 2020 Elsevier.

In another contribution, Zhang *et al.* developed a novel paper@QDs@MIPs fluorescence sensor to detect 2,4-D based on electron-transfer-induced fluorescence quenching.[258] This sensor is inexpensive with a lower recognition rate and detection limit of 0.12 μM. Wang *et al.* and Xu *et al.* constructed a novel "signal-on" type MIP-based ratiometric fluorescence sensor which detects 2,4-D by using nitrobenzoxadiazole (NBD) and QD@SiO_2 as a core.[259–261] The proposed sensor showed a high sensitivity for 2,4-D with a low LoD (0.13 μM) (Fig. 31). By using electron transfer to cause the fluorescence quenching, Xu *et al.* have created a novel MOF-based probe, such as the Mg(II) complex containing 4,4′-(4-aminopyridine-3,5-diyl)dibenzoic acid, that can detect electron-deficient 2,6-dichloro-4-nitroaniline (DCN).[261] The probe showed good selectivity towards DCN in the presence of other pesticides and the LoD was found to be 150 ppb. Xu *et al.* have developed a Cd-LMOF complex by reacting a rigid conjugated tricarboxylic acid ligand 4,4′-(9-(4′-carboxy-[1,1′-biphenyl]-4-yl)-9*H*-carbazole-3,6-diyl)dibenzoic acid (H_3CBCD) with Cd(II), which showed a strong blue fluorescent emission.[262,263] The synthesized complex was used to detect DCN *via* electron transfer. Besides PET, the resonance energy transfer contributes to the observed fluorescent quenching.

Guo *et al.* have synthesized a 2D Zn-based MOF containing 4-(tetrazol-5-yl)phenyl-4,2′:6′,4″-terpyridine and terephthalic acid as the ligand with blue fluorescence for the detection of DCN and the LoD was found to be 1.90 μM.[263,264] Tao *et al.* have reported a Zn-based luminescent MOF appended (*E*)-1,2-diphenyl-1,2-bis(4-(pyridin-4-yl)phenyl) ethene to detect DCN with AIE properties.[264,265] In 2019, Wang *et al.* developed a novel MOF Zn(II) complex of 3,5-di(2′,4′-dicarboxylphenyl)benzoic acid and 1,2-di(4-pyridyl)ethylene by the solvothermal method to detect the presence of 2,6-dichloro-4-nitroaniline with low detection limits in aqueous solution.[266] In another study, Chi *et al.* reported carboxylic acid substituent appended Zn-based coordination polymers for 2,6-dichloro-4-nitroaniline detection.[267] A copper-based MOF containing the 4,4′-bipyridine and succinate dianion has been developed and studied using theoretical density functional theory analysis. This research shows that the MOF may selectively detect

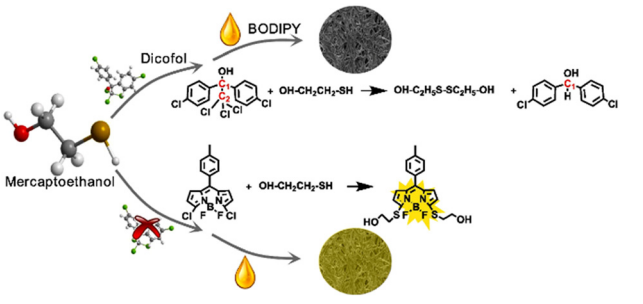

Fig. 32 Proposed reaction mechanism of mercaptoethanol with dicofol and BODIPY. Reprinted with permission from ref. 270. Copyright 2022 Elsevier.

pesticides similar to atrazine and dicofol.[247] The Feng group developed a novel two-dimensional (2D) cadmium-based MOF for the detection of DCN due to PET and FRET.[268]

Sharma and coworkers synthesized a fluorescent supramolecular assembly based on anthracene/perylene bisamide (PBI) derivatives to detect the presence of organophosphate (CPF) and organochlorine (DCN) pesticides in aqueous media by the inner filter effect for the "on–off" detection of DCN.[269] In addition, researchers have investigated the practical uses of supramolecular assemblies for detecting CPF and DCN in contaminated water and agricultural products, including grapes and apples. To detect dicofol, Wang *et al.* developed a fluorometric chemosensor based on mercaptoethanol and boron dipyrromethene (BODIPY) (Fig. 32). A 'turn-off' fluorescence behavior was noticed upon reaction with dicofol and a detection limit of 200 ppb.[270] Two ternary Cd(II) coordination polymers$\{[Cd(tptc)0.5(bpz)(H_2O)]\cdot 0.5H_2O\}_n$ (CP1) and $[Cd(tptc)0.5(bpy)]_n$ (CP2) were designed through the mixed ligand strategy.[271] Two Cd(II) coordination polymers (CPs) exhibit remarkable chemical stability and luminescence properties. These CPs demonstrate efficient multi-functional fluorescent responses towards dichloro-4-nitroaniline in aqueous media. The detection limits for CP1 and CP2 are 112 ppb and 638 ppb, respectively. Table 5 summarizes the fluorescent sensing properties of several sensors for organochlorine pesticide detection.

4.6 Fluorescence sensing of neonicotinoid pesticides

The discovery of neonicotinamides, a new class of insecticides, marks a significant advancement in pesticide research in recent years. They specifically affect the central nervous system of insects by acting as an antagonist of their molecular target site, the post-synaptic nicotinic receptors (nAChRs). Neonicotinamide pesticides are an emerging contaminant, hence it is crucial to identify and eliminate them. A new fluorescent probe, ZnS:Mn-aptamer, has been developed using quantum dots (QDs) for acetamiprid visual detection.

The fluorescence of the sensor was quenched by the FRET between the multi-walled carbon nanotubes (MWCNTs) and ZnS:Mn-aptamer. When acetamiprid was added, preferential binding with ZnS:Mn-aptamer took place which caused a reduction in FRET and thereby turning on the fluorescence.[272,273] Hu *et al.* reported a new nanosensor based on aptamers for the detection of acetamiprid utilizing FRET between NH_2-$NaYF_4$:Yb, holmium silica dioxide (Ho@SiO_2) up-conversion NPs (UCNPs) and AuNPs.[274] A colorimetric and fluorometric approach involving an acetamiprid-binding aptamer (ABA), AuNPs, and UCNPs was employed for the ultrasensitive and selective detection of acetamiprid. The ABA underwent a structural switch from a DNA duplex to an aptamer–acetamiprid complex and also dissociated from the AuNPs. The dual approach used the principles of salt-induced AuNP aggregation, analyte-triggered structural switch of aptamers, and UCNP signal amplification.[275]

An AuNPs-QDs system caused a fluorescent quenching of RF-QDs induced by combining ratiometric fluorescent QDs (RF-QDs) with AuNPs due to IFE (Fig. 33). The interaction of acetamiprid with AuNPs exhibited a change of color from purple to dark blue due to aggregation.[250] An imprinted fluorescent nanoprobe based on SiO_2-coated NaYF4:Yb, Er UCNPs encapsulated with an MIP has been fabricated for acetamiprid detection. The fluorescence of UCNP@MIP was suppressed when combined with acetamiprid, due to photo-

Table 5 Summary of fluorescence sensing properties of various sensors for organochlorine pesticide detection

Probe	Analyte	LoD	Ref.
Glutathione coated CdS (GSH-CdS) QDs	Dicofol	55 ± 11 ppb	253
Methylammonium lead halide perovskite quantum dots (MAPB-QDs)	pentachlorophenol	0.02 μM	254
Mn-doped ZnS QDs-MIPs	pentachlorophenol	86 nM	255
Mn-doped ZnS QDs-Fe_3O_4 nanoparticles	pentachlorophenol	0.5 μmol L^{-1}	256
GQDs-CdS nanocrystals	pentachlorophenol	3 pg m L^{-1}	257
Mesoporous structured imprinting microspheres on the surfaces of quantum dots (QDs)	2,4-D	2.1 nM	258
Paper@QDs@MIPs	2,4-D	90 nM	259
Nitrobenzoxadiazole (NBD) and QD@SiO_2	2,4-D	0.14 μM	261
Mg(II) complex containing 4,4′-(4-aminopyridine-3,5-diyl)dibenzoic acid	2,6-Dichloro-4-nitroaniline	150 ppb	262
$[Cd_3(CBCD)_2(DMA)_4(H_2O)_2]\cdot 10DMA$ (Cd-CBCD). Cd-CBCD	2,6-Dichloro-4-nitroaniline	145 ppb	263
Zn-based MOF containing 4-(tetrazol-5-yl)phenyl-4,2′:6′,4″-terpyridine and terephthalic acid	2,6-Dichloro-4-nitroaniline	1.90 μM	265
Zn(II) complex of (*E*)-1,2-diphenyl-1,2-bis(4-(pyridin-4-yl)phenyl)ethene	2,6-Dichloro-4-nitroaniline	0.13 ppm	264
Zn(II) complex of 3,5-di(2′,4′-dicarboxylphenyl)benzoic acid and 1,2-di(4-pyridyl)ethylene	2,6-Dichloro-4-nitroaniline	~166 ppb	266
Zn-based coordination polymers	2,6-Dichloro-4-nitroaniline	6.7×10^{-5} M^{-1} (CP1) & 2.8×10^{-5} M^{-1} (CP2)	267
Cd-based metal–organic framework	2,6-Dichloro-4-nitroaniline	0.221 ppm	268
Anthracene/perylene bisamide (PBI) derivatives	Chlorpyrifos & DCN	0.10×10^{-7} M^{-1} & 0.18 nM	269
Mercaptoethanol and boron dipyrromethene	Dicofol	200 ppb	270
Cd(II) coordination polymers	2,6-Dichloro-4-nitroaniline	112 ppb (CP1) & 638 ppb (CP2)	271

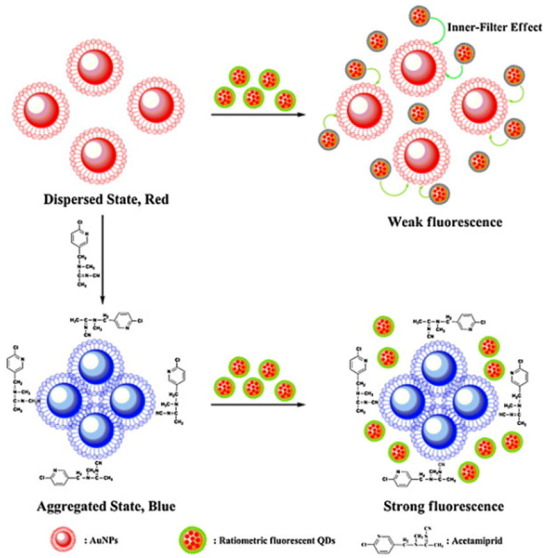

Fig. 33 The fluorescent detection of acetamiprid through the inner-filter effect of gold nanoparticles on QDs. Reprinted with permission from ref. 276. Copyright 2014 Elsevier.

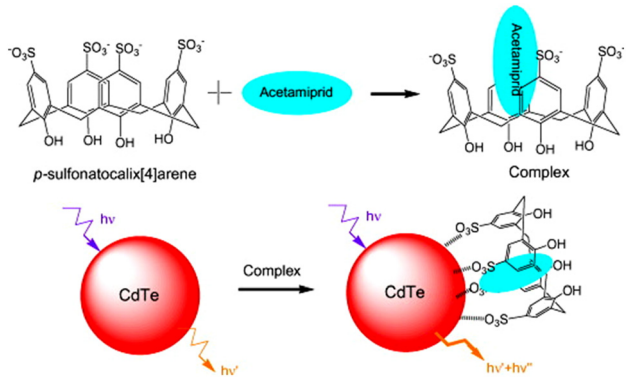

Fig. 34 Host–guest complexation of acetamiprid enhances the fluorescence of CdTe QDs in the presence of *p*-sulfonatocalix[4]arene. Reprinted with permission from ref. 278. Copyright 2009 Elsevier.

induced electron transfer. The detection limit for this combination was 8.3 ng mL^{-1}. The approach was effectively adopted acetamiprid detection in apple and strawberry samples, yielding recoveries ranging from 89.6% to 97.9%.[276] A MIP based on silane-doped carbon dots (Si–CDs) has been developed as a probe for acetamiprid (ACT) detection with high selectivity. The fluorescence signal of MIP@Si–CDs displayed a detection limit of 2 nM and utilized ACT detection in real samples.[277] Qu *et al.* utilized the ability of calixarene to bind fenamithion and acetamiprid to sufficiently remove these pesticides from the proximity of the QDs and restore their fluorescence (Fig. 34).[278] It has been found that imidacloprid significantly quenches the fluorescence of poly-(2,6-dimethoxynaphthalene).[279] Scientists combined MOFs with luminescent indicators to identify and degrade nitenpyram (NIT). Fluorescent probes for MOFs were created using porphyrin fluorophores. The probe experienced electron transfer under the influence of NIT, leading to the suppression of fluorescence.[280] Liu *et al.* developed a test strip-based fluorescent sensor for thiacloprid based on polydopamine (PDA) MIPs and N-GQDs. Thiacloprid was selectively captured *via* PDA-MIP, increasing the fluorescence intensity of N-GQDs. This increase in intensity was directly proportional to the concentration of thiacloprid within the range of 0.1–10 mg L^{-1}. The limit of detection for thiacloprid was found to be 0.03 mg L^{-1}, which is rather low.[281] Table 6 summarizes the fluorescence sensing properties of various fluorescent sensors for neonicotinoid pesticide detection.

5. Conclusions and outlook

In summary, we have exemplified in detail the chemosensing applications of fluorescence materials reported so far to detect various classes of structurally assorted pesticides. We have systematically categorized pesticides into several groups depending upon their structures and functions and each section highlights the fluorescence sensing properties of different sensors for the detection of a particular class of pesticides including their mechanism of fluorescence sensing, selectivity, and sensitivity for detection (see Tables 1–6 for further details). At the beginning of this review, we have discussed the classification of pesticides, different detection methods currently available for pesticide detection, and fluorescence-based sensing mechanisms proposed for pesticide detection. In the later part, a detailed

Table 6 Summary of fluorescence sensing properties of various sensors for neonicotinoid pesticide detection

Probe	Analyte	LoD	Ref.
ZnS:Mn aptamer quantum dots	Acetamiprid	0.7 nM	272
CdTe quantum dots-AuNPs	Acetamiprid	7.29 nM	273
NH_2-$NaYF_4$:Yb, holmium silica dioxide (Ho@SiO_2) UCNPs and AuNPs	Acetamiprid	3.2 nM	274
AuNPs-upconversion nanoparticles	Acetamiprid	0.36 nm	275
RF quantum dots-AuNPs	Acetamiprid	16.8 μg L^{-1}	250
SiO_2-coated $NaYF_4$:Yb, Er upconversion nanoparticles (UCNP)-IPs	Acetamiprid	8.3 ng mL^{-1}	276
MIP@Si–CDs	Acetamiprid	2 nM	277
CdTe (QDs)-*p*-sulfonatocalix[4]arene	Fenamithion and acetamiprid	1.2×10^{-8} M (fenamithion) and 3.4×10^{-8} M (acetamiprid)	278
Poly(2,6-dimethoxynaphthalene) based probe	Imidacloprid	3.093 ng mL^{-1}	279
Bifunctional nanoscale porphyrinic MOF probe	Nitenpyram	0.03 μg mL^{-1}	280
Nitrogen-doped graphene QDs (GQDs)	Thiacloprid	0.03 mg L^{-1}	281

report on various fluorescence-based sensing materials for different types of pesticides is provided. The evolution of fluorescence-based sensing materials is a topical area of research and is at the forefront of the materials sciences. The fluorescence-based sensing methods have different ways of finding innovative materials for efficiently sensing various analytes. The selectivity of materials can be tailored to specifically target particular analytes in complex sample matrices, and sensing capability can be improved by linking individual binding units into the polymeric network that supplies a large number of binding sites for detection and thus, significant enhancement in sensitivity of materials. The real-time utility of fluorescence-based sensors for pesticide detection is, however, limited by several issues and difficulties that need to be fixed to realize their useful applications, even with the notable advancement.

Most of the sensor systems/molecules discussed herein detect pesticides through a fluorescence quenching mechanism, except in a few cases where the binding of pesticides enhances the fluorescence intensity of sensors. In general, it is proclaimed that fluorescence turn-on sensing would be more beneficial because the naked eye can easily visualize the sensing. The other challenge is that the current methodologies have been established by detecting a single analyte, but numerous real-time samples contain a mixture of pesticides. Therefore, the design of suitable sensors with discriminating capability would be appealing. Moreover, on-site analysis can resolve the environmental impact of these pesticides. Another notable issue with the reported sensors is their poor stability in real-time sensing media such as stability under aqueous conditions and under varied pH ranges. Hence, a collective detection of pesticide residues that can enable on-site determination has to be demonstrated. An alternative strategy could be thought from the use of remote-operated sensors. Moreover, systematic studies are necessary for better understanding the interactions between sensors and pesticides because there is a substantial absence of knowledge on the precise mechanism of fluorescence sensing for several of the sensors covered in this review. According to the review's findings, many areas require more study to create and build workable fluorescence-based sensor systems for real-time pesticide detection. Given the information above, we encourage researchers to develop a sustainable method of detecting pesticides that overcomes present obstacles and relies on fluorescence sensing to improve the environment.

This review article provides a detailed report on fluorescence chemosensors reported to date for structurally assorted classes of pesticide detection. Particular emphasis has been dedicated to the sensing mechanism, sensitivity, mode of binding, and efficient sensing of pesticides in real samples. We also highlighted the current challenges with the existing sensors and the perspective on addressing these challenges to develop practically useful sensor systems for pesticide detection. We strongly believe that this review will inspire researchers working in the related areas to find suitable fluorescent-based sensors for real-time monitoring of pesticides.

Data availability

No primary research results, software, or code have been included and no new data were generated or analyzed as part of this review.

Author contributions

G. Kalaiarasi: conceptualization, software, resources, visualization, funding acquisition, writing – original draft; Y. Jegadeesan: software, resources, visualization, writing – original draft; A. Shanmughan: software, resources, visualization, writing – original draft; M. K. Noushija: software, resources, visualization, writing – review & editing; A. V. Krishna: software, resources, visualization, writing – review & editing; H. Gangadharan: software, resources, visualization, writing – review & editing; D. Umadevi: conceptualization, software, resources, visualization, supervision, investigation, project administration, funding acquisition, writing – review & editing; S. Shanmugaraju: conceptualization, software, resources, visualization, project administration, supervision, investigation, funding acquisition, writing – original draft, writing – review & editing.

Conflicts of interest

There are no conflicts to declare.

Acknowledgements

The authors thank the Indian Institute of Technology Palakkad (ERG research grant 2023-168-CHY-SHS-ERG-SP to SS) and the Science and Engineering Research Board (EMEQ research grant EEQ/2023/000386 to S.S.), India, for financial support. D. U. thanks DST India for funding (DST/WOS-A/CS-68/2021). G. K. sincerely thanks the Tamil Nadu State Council for Science and Technology (TNSCST) for the Young Scientist Fellowship.

References

1 R. Repetto and S. Baliga, Trends and patterns of pesticide use: in *Pesticides and the immune system; Public Health Risks*, World Resources Institute, Washington, D.C., 1996, pp. 3–8.
2 J. T. Zacharia, *Pestic. Mod. world-trends Pestic. Anal.*, 2011, pp. 1–18.
3 I. C. Yadav, N. L. Devi, J. H. Syed, Z. Cheng, J. Li, G. Zhang and K. C. Jones, *Sci. Total Environ.*, 2015, **511**, 123–137.
4 S. Savary, L. Willocquet, S. J. Pethybridge, P. Esker, N. McRoberts and A. Nelson, *Nat. Ecol. Evol.*, 2019, **3**, 430–439.
5 S. A. Nsibande and P. B. C. Forbes, *Anal. Chim. Acta*, 2016, **945**, 9–22.
6 Y. Abubakar, H. Tijjani, C. Egbuna, C. O. Adetunji, S. Kala, T. L. Kryeziu, J. C. Ifemeje and K. C. Patrick-Iwuanyanwu, in *Natural remedies for pest, disease and weed control*, Elsevier, 2020, pp. 29–42.

7 M. A. Rodrigo, N. Oturan and M. A. Oturan, *Chem. Rev.*, 2014, **114**, 8720–8745.
8 E.-C. Oerke, *J. Agric. Sci.*, 2006, **144**, 31–43.
9 A. Samsidar, S. Siddiquee and S. M. Shaarani, *Trends Food Sci. Technol.*, 2018, **71**, 188–201.
10 Canadian Cancer Society, Cosmetic Pesticides. Information Brief, 2013.
11 W. Mnif, A. I. H. Hassine, A. Bouaziz, A. Bartegi, O. Thomas and B. Roig, *Int. J. Environ. Res. Public Health*, 2011, **8**, 2265–2303.
12 D. Goulson, *Nature*, 2014, **511**, 295–296.
13 S. Zheng, B. Chen, X. Qiu, M. Chen, Z. Ma and X. Yu, *Chemosphere*, 2016, **144**, 1177–1192.
14 J. Römbke, R. M. Schmelz and C. Pelosi, *Front. Environ. Sci.*, 2017, **5**, 20.
15 M. Pirsaheb, M. Limoee, F. Namdari and R. Khamutian, *Med. J. Islam. Repub. Iran*, 2015, **29**, 228.
16 G.-E. Séralini, E. Clair, R. Mesnage, S. Gress, N. Defarge, M. Malatesta, D. Hennequin and J. S. de Vendômois, *Environ. Sci. Eur.*, 2014, **26**, 1–17.
17 D. S. Thakur, R. Khot, P. P. Joshi, M. Pandharipande and K. Nagpure, *Toxicol. Int.*, 2014, **21**, 328.
18 J. K. Sathish Kumar, S. S. Monica, B. Vinothkumar, A. Suganthi and M. Paramasivam, *Agricultural Reviews*, 2024, **45**, R-2325.
19 E. Reiler, E. Jørs, J. Bælum, O. Huici, M. M. A. Caero and N. Cedergreen, *Sci. Total Environ.*, 2015, **527**, 262–269.
20 A. Witczak and H. Abdel-Gawad, *J. Environ. Sci. Health, Part B*, 2014, **49**, 917–928.
21 S. Chourasiya, P. S. Khillare and D. S. Jyethi, *Environ. Sci. Pollut. Res.*, 2015, **22**, 5793–5806.
22 C. Buscail, C. Chevrier, T. Serrano, F. Pelé, C. Monfort, S. Cordier and J.-F. Viel, *Occup. Environ. Med.*, 2015, **72**, 837–844.
23 D. Lu, D. Wang, R. Ni, Y. Lin, C. Feng, Q. Xu, X. Jia, G. Wang and Z. Zhou, *Environ. Sci. Pollut. Res.*, 2015, **22**, 9293–9306.
24 E. Homburg and E. Vaupel, *Hazardous Chemicals: Agents of Risk and Change, 1800–2000*, Berghahn Books, 2019, vol. 17.
25 N. C. Deziel, J. L. Warren, H. Huang, H. Zhou, A. Sjodin and Y. Zhang, *Environ. Res.*, 2021, **192**, 110333.
26 P. Booij, I. Holoubek, J. Klánová, J. Kohoutek, A. Dvorská, K. Magulová, S. Al-Zadjali and P. Čupr, *Sci. Total Environ.*, 2016, **550**, 231–240.
27 G. L. Daly, Y. D. Lei, C. Teixeira, D. C. G. Muir, L. E. Castillo, L. M. M. Jantunen and F. Wania, *Environ. Sci. Technol.*, 2007, **41**, 1124–1130.
28 M. J. Adkesson, J. M. Levengood, J. W. Scott, D. J. Schaeffer, J. N. Langan, S. Cárdenas-Alayza, S. De La Puente, P. Majluf and S. Yi, *J. Wildl. Dis.*, 2018, **54**, 304–314.
29 L. Hunt, C. Bonetto, V. H. Resh, D. F. Buss, S. Fanelli, N. Marrochi and M. J. Lydy, *Sci. Total Environ.*, 2016, **547**, 114–124.
30 P. E. Davies, L. S. J. Cook and J. L. Barton, *Aust. J. Mar. Freshwater Res.*, 1994, **45**, 209–226.
31 E. De Gerónimo, V. C. Aparicio, S. Bárbaro, R. Portocarrero, S. Jaime and J. L. Costa, *Chemosphere*, 2014, **107**, 423–431.
32 F. P. Carvalho, J.-P. Villeneuve, C. Cattini, J. Rendón and J. M. de Oliveira, *Chemosphere*, 2009, **74**, 988–995.
33 H. De Bon, J. Huat, L. Parrot, A. Sinzogan, T. Martin, E. Malezieux and J.-F. Vayssières, *Agron. Sustainable Dev.*, 2014, **34**, 723–736.
34 B. K. Singh and A. Walker, *FEMS Microbiol. Rev.*, 2006, **30**, 428–471.
35 C. Potera, Agriculture: Pesticides disrupt nitrogen fixation, *Environ. Health Perspect.*, 2007, **115**, A579.
36 I. C. Yadav and N. L. Devi, *Environ. Sci. Eng.*, 2017, **6**, 140–158.
37 M. C. R. Alavanja, C. Samanic, M. Dosemeci, J. Lubin, R. Tarone, C. F. Lynch, C. Knott, K. Thomas, J. A. Hoppin and J. Barker, *Am. J. Epidemiol.*, 2003, **157**, 800–814.
38 Z.-Q. Jia, Y.-C. Zhang, Q.-T. Huang, A. K. Jones, Z.-J. Han and C.-Q. Zhao, *J. Hazard. Mater.*, 2020, **394**, 122521.
39 H. Guan, W. E. Brewer, S. T. Garris and S. L. Morgan, *J. Chromatogr. A*, 2010, **1217**, 1867–1874.
40 Y. Fu, X. Dou, L. Zhang, J. Qin, M. Yang and J. Luo, *J. Chromatogr., B*, 2019, **1125**, 121730.
41 R. Mondal, A. Mukherjee, S. Biswas and R. K. Kole, *Chemosphere*, 2018, **206**, 217–230.
42 A. Stachniuk, A. Szmagara, R. Czeczko and E. Fornal, *J. Environ. Sci. Health, Part B*, 2017, **52**, 446–457.
43 W. Gui, C. Tian, Q. Sun, S. Li, W. Zhang, J. Tang and G. Zhu, *Water Res.*, 2016, **95**, 185–194.
44 F. Arduini, S. Cinti, V. Caratelli, L. Amendola, G. Palleschi and D. Moscone, *Biosens. Bioelectron.*, 2019, **126**, 346–354.
45 Y. Li, Q. Luo, R. Hu, Z. Chen and P. Qiu, *Chin. Chem. Lett.*, 2018, **29**, 1845–1848.
46 S. Chen, Y.-L. Yu and J.-H. Wang, *Anal. Chim. Acta*, 2018, **999**, 13–26.
47 A. Bigdeli, F. Ghasemi, S. Abbasi-Moayed, M. Shahrajabian, N. Fahimi-Kashani, S. Jafarinejad, M. A. F. Nejad and M. R. Hormozi-Nezhad, *Anal. Chim. Acta*, 2019, **1079**, 30–58.
48 S. Shanmugaraju and P. S. Mukherjee, *Chem. Commun.*, 2015, **51**, 16014–16032; X. Yan, H. Li and X. Su, *TrAC, Trends Anal. Chem.*, 2018, **103**, 1–20.
49 R. Singh, P. Thakur, A. Thakur, H. Kumar, P. Chawla, J. V. Rohit, R. Kaushik and N. Kumar, *Int. J. Environ. Anal. Chem.*, 2021, **101**, 3006–3022.
50 G. K. Mishra, V. Sharma and R. K. Mishra, *Biosensors*, 2018, **8**, 28.
51 N. Serio, J. Roque, A. Badwal and M. Levine, *Analyst*, 2015, **140**, 7503–7507.
52 S. Farooq, J. Nie, Y. Cheng, Z. Yan, J. Li, S. A. S. Bacha, A. Mushtaq and H. Zhang, *Analyst*, 2018, **143**, 3971–3989.
53 S. K. Panigrahi and A. K. Mishra, *J. Photochem. Photobiol., C*, 2019, **41**, 100318.
54 D. Cao, L. Zhu, Z. Liu and W. Lin, *J. Photochem. Photobiol., C*, 2020, **44**, 100371.
55 L. Wu, C. Huang, B. P. Emery, A. C. Sedgwick, S. D. Bull, X.-P. He, H. Tian, J. Yoon, J. L. Sessler and T. D. James, *Chem. Soc. Rev.*, 2020, **49**, 5110–5139.
56 M. Levine, *Front. Chem.*, 2021, **9**, 616815; T. Skorjanc, D. Shetty and M. Valant, *ACS Sens.*, 2021, **6**, 1461–1481; H.

Bhambri, S. Khullar, Sakshi and S. K. Mandal, *Mater. Adv.*, 2022, **3**, 19–124.
57 M. A. Hassaan and A. El Nemr, *Egypt. J. Aquat. Res.*, 2020, **46**, 207–220.
58 K. H. Büchel, *Chemistry of pesticides*, Wiley New York, New York, 1983, p. 518.
59 E. J. Mrema, F. M. Rubino, G. Brambilla, A. Moretto, A. M. Tsatsakis and C. Colosio, *Toxicology*, 2013, **307**, 74–88.
60 S. Ragab, A. El Sikaily and A. El Nemr, *Egypt. J. Aquat. Res.*, 2016, **42**, 365–374.
61 L. Gámiz-Gracia, A. M. García-Campaña, J. J. Soto-Chinchilla, J. F. Huertas-Pérez and A. González-Casado, *TrAC, Trends Anal. Chem.*, 2005, **24**, 927–942.
62 C. Bolognesi, *Mutat. Res., Rev. Mutat. Res.*, 2003, **543**, 251–272.
63 A. Vale and M. Lotti, *Handb. Clin. Neurol.*, 2015, **131**, 149–168.
64 A. El Nemr and M. M. El-Sadaawy, *Int. J. Sediment Res.*, 2016, **31**, 44–52.
65 A. El Nemr, G. F. El-Said and A. Khaled, *Water Environ. Res.*, 2016, **88**, 325–337.
66 E. L. Robb, A. C. Regina and M. B. Baker, *Organophosphate Toxicity*, StatPearls Publishing, Treasure Island, Florida, 2024.
67 F. P. Garcia, S. Y. C. Ascencio, J. C. G. Oyarzún, A. C. Hernandez and P. V. Alavarado, *Journal of Research in Environmental Science and Technology*, 2012, **1**, 279–293.
68 J. R. Reigart, *Recognition and management of pesticide poisonings*, DIANE Publishing, 2009.
69 R. C. Gupta and J. W. Crissman, in *Haschek and Rousseaux's Handbook of Toxicologic Pathology*, Elsevier, 2013, pp. 1349–1372.
70 S. Saari, A. Näreaho and S. Nikander, *Canine parasites and parasitic diseases*, Academic Press, 2018.
71 F. M. Fishel and J. A. Ferrell, Managing Pesticide Drift, **https://edis.ifas.ufl.edu/publication/PI232**.
72 D. Li, M. He, B. Chen and B. Hu, *J. Chromatogr. A*, 2019, **1583**, 19–27.
73 R. Umapathi, S. Sonwal, M. J. Lee, G. M. Rani, E.-S. Lee, T.-J. Jeon, S.-M. Kang, M.-H. Oh and Y. S. Huh, *Coord. Chem. Rev.*, 2021, **446**, 214061.
74 R. Singh, N. Kumar, R. Mehra, H. Kumar and V. P. Singh, *Trends Environ. Anal. Chem.*, 2020, **26**, e00086.
75 P. Chawla, R. Kaushik, V. J. S. Swaraj and N. Kumar, *Environ. Nanotechnol., Monit. Manage.*, 2018, **10**, 292–307.
76 H. Patel, D. Rawtani and Y. K. Agrawal, *Trends Food Sci. Technol.*, 2019, **85**, 78–91.
77 M. Liu, A. Khan, Z. Wang, Y. Liu, G. Yang, Y. Deng and N. He, *Biosens. Bioelectron.*, 2019, **130**, 174–184.
78 I. S. Che Sulaiman, B. W. Chieng, M. J. Osman, K. K. Ong, J. I. A. Rashid, W. M. Z. Wan Yunus, S. A. M. Noor, N. A. M. Kasim, N. A. Halim and A. Mohamad, *Microchim. Acta*, 2020, **187**, 1–22.
79 G. M. Fernandes, W. R. Silva, D. N. Barreto, R. S. Lamarca, P. C. F. L. Gomes, J. F. da S. Petruci and A. D. Batista, *Anal. Chim. Acta*, 2020, **1135**, 187–203; Z.-L. Li, X.-R. Qi, Y.-H. Xu, J.-Q. Zhao, G.-F. Zuo and M.-M. Wang, *Food Chem.*, 2025, **472**, 142904.
80 M. Bhattu, M. Verma and D. Kathuria, *Anal. Methods*, 2021, **13**, 4390–4428.
81 P. Shah, X. Zhu and C. Li, *Expert Rev. Mol. Diagn.*, 2013, **13**, 83–91.
82 F. Li, M. You, S. Li, J. Hu, C. Liu, Y. Gong, H. Yang and F. Xu, *Biotechnol. Adv.*, 2020, **39**, 107442.
83 R. Jin, L. Zhao, X. Yan, X. Han, M. Liu, Y. Chen, Q. Li, D. Su, F. Liu and P. Sun, *Biosens. Bioelectron.*, 2020, **167**, 112457.
84 P. N. Minh, V.-T. Hoang, N. X. Dinh, O. Van Hoang, N. Van Cuong, D. T. B. Hop, T. Q. Tuan, N. T. Khi, T. Q. Huy and A.-T. Le, *New J. Chem.*, 2020, **44**, 7611–7620.
85 M.-G. Lee, V. Patil, Y.-C. Na, D. S. Lee, S. H. Lim and G.-R. Yi, *Sens. Actuators, B*, 2018, **261**, 489–496.
86 J. Wei, L. Yang, M. Luo, Y. Wang and P. Li, *Ecotoxicol. Environ. Saf.*, 2019, **179**, 17–23.
87 S. A. Ghoto, M. Y. Khuhawar, T. M. Jahangir and J. ul D. Mangi, *J. Nanostruct. Chem.*, 2019, **9**, 77–93.
88 S. A. Ghoto, M. Y. Khuhawar and T. M. Jahangir, *Anal. Sci.*, 2019, **35**, 631–637.
89 M. M. Bordbar, T. A. Nguyen, F. Arduini and H. Bagheri, *Microchim. Acta*, 2020, **187**, 1–13.
90 M. M. Bordbar, T.-A. Nguyen, A. Q. Tran and H. Bagheri, *Sci. Rep.*, 2020, **10**, 17302.
91 J. Kaur and P. K. Singh, *Phys. Chem. Chem. Phys.*, 2020, **22**, 15105–15119.
92 Z. Sun, L. Tian, M. Guo, X. Xu, Q. Li and H. Weng, *Food Control*, 2017, **81**, 23–29.
93 M. E. I. Badawy and A. F. El-Aswad, *Int. J. Anal. Chem.*, 2014, 536823.
94 M. Kavruk, V. C. Özalp and H. A. Öktem, *J. Anal. Methods Chem.*, 2013, 932946.
95 S. Uniyal and R. K. Sharma, *Biosens. Bioelectron.*, 2018, **116**, 37–50.
96 R. Zamora, F. Masís-Meléndez, H. Phillips, L. A. Alvarado-Marchena and R. Starbird, *Int. J. Electrochem. Sci.*, 2018, **13**, 1931–1944.
97 F. Della Pelle, C. Angelini, M. Sergi, M. Del Carlo, A. Pepe and D. Compagnone, *Talanta*, 2018, **186**, 389–396.
98 X. Tu, F. Gao, X. Ma, J. Zou, Y. Yu, M. Li, F. Qu, X. Huang and L. Lu, *J. Hazard. Mater.*, 2020, **396**, 122776.
99 C. Gu, Q. Wang, L. Zhang, P. Yang, Y. Xie and J. Fei, *Sens. Actuators, B*, 2020, **305**, 127478.
100 Y. Bakytkarim, S. Tursynbolat, Q. Zeng, J. Huang and L. Wang, *J. Electroanal. Chem.*, 2019, **841**, 45–50.
101 J. P. Giraldo, H. Wu, G. M. Newkirk and S. Kruss, *Nat. Nanotechnol.*, 2019, **14**, 541–553.
102 F. Zhao, J. He, X. Li, Y. Bai, Y. Ying and J. Ping, *Biosens. Bioelectron.*, 2020, **170**, 112636.
103 Z. Usmani, M. Sharma, A. K. Awasthi, G. D. Sharma, D. Cysneiros, S. C. Nayak, V. K. Thakur, R. Naidu, A. Pandey and V. K. Gupta, *J. Hazard. Mater.*, 2021, **416**, 126154.
104 H. Teymourian, M. Parrilla, J. R. Sempionatto, N. F. Montiel, A. Barfidokht, R. Van Echelpoel, K. De Wael and J. Wang, *ACS Sens.*, 2020, **5**, 2679–2700.
105 X. Yang and H. Cheng, *Micromachines*, 2020, **11**, 243.

106 D. Zhang, J. Jiang, J. Chen, Q. Zhang, Y. Lu, Y. Yao, S. Li, G. L. Liu and Q. Liu, *Biosens. Bioelectron.*, 2015, **70**, 81–88.
107 K. Xu, Q. Chen, Y. Zhao, C. Ge, S. Lin and J. Liao, *Sens. Actuators, B*, 2020, **319**, 128221.
108 D. Ji, Z. Shi, Z. Liu, S. S. Low, J. Zhu, T. Zhang, Z. Chen, X. Yu, Y. Lu and D. Lu, *Smart Mater. Med.*, 2020, **1**, 1–9.
109 B. B. Campos, R. Contreras-Cáceres, T. J. Bandosz, J. Jiménez-Jiménez, E. Rodríguez-Castellón, J. C. G. E. da Silva and M. Algarra, *Sens. Actuators, B*, 2017, **239**, 553–561; N. Zhou, M. Cai, S. Zheng, H. Guo and F. Yang, *Sens. Actuators, B*, 2017, **417**, 136051.
110 Y. Hao, Q. Yin, Y. Zhang, M. Xu and S. Chen, *Molecules*, 2019, **24**, 3716; P. He, Y. Chen, L. Lin, H. Guo and F. Yang, *Talanta*, 2024, **276**, 126269.
111 S. Goswami, S. Cekli, E. Alarousu, R. W. Winkel, M. Younus, O. F. Mohammed and K. S. Schanze, *Macromolecules*, 2020, **53**, 6279–6287.
112 T. T. Vu, T. N. N. Dau, C. T. Ly, D. C. Pham, T. T. N. Nguyen and V. T. Pham, *J. Mater. Sci.*, 2020, **55**, 9070–9081.
113 J. Chen, X. Chen, Q. Huang, W. Li, Q. Yu, L. Zhu, T. Zhu, S. Liu and Z. Chi, *ACS Appl. Mater. Interfaces*, 2019, **11**, 32689–32696.
114 X. Li, W. Ma, H. Li, Q. Zhang and Z. Ma, *Trends Food Sci. Technol.*, 2020, **97**, 185–195.
115 S.-L. Yang, J.-N. Lu, S.-J. Zhang, C.-X. Zhang and Q.-L. Wang, *Analyst*, 2018, **143**, 4901–4906.
116 P.-L. Champagne, R. Kumar and C.-C. Ling, *Sens. Actuators, B*, 2019, **281**, 229–238.
117 T. Tian, F. Qiu, K. Dong and D. Yang, *Toxicol. Environ. Chem.*, 2012, **94**, 1034–1042.
118 C. Jiang, Z. Song, L. Yu, S. Ye and H. He, *TrAC, Trends Anal. Chem.*, 2020, **133**, 116086.
119 M. Ganesan and P. Nagaraaj, *Anal. Methods*, 2020, **12**, 4254–4275.
120 A. Mehta, A. Mishra, S. Basu, N. P. Shetti, K. R. Reddy, T. A. Saleh and T. M. Aminabhavi, *J. Environ. Manage.*, 2019, **250**, 109486.
121 P. C. Dey and R. Das, *Spectrochim. Acta, Part A*, 2019, **207**, 156–163.
122 M. Lasagna, M. S. Hielpos, C. Ventura, M. N. Mardirosian, G. Martín, N. Miret, A. Randi, M. Núñez and C. Cocca, *Ecotoxicol. Environ. Saf.*, 2020, **205**, 111312.
123 M. A. Ghasemzadeh, B. Mirhosseini-Eshkevari, M. Tavakoli and F. Zamani, *Green Chem.*, 2020, **22**, 7265–7300.
124 D. Y. Heo, H. H. Do, S. H. Ahn and S. Y. Kim, *Polymers*, 2020, **12**, 2061.
125 J. Kaushal, M. Khatri and S. K. Arya, *Ecotoxicol. Environ. Saf.*, 2021, **207**, 111483.
126 T. C. Kwong, *Ther. Drug Monit.*, 2002, **24**, 144–149.
127 R. Cochran, in *Hayes' Handbook of Pesticide Toxicology*, Elsevier, 2010, pp. 337–355.
128 K. Vikrant, D. C. W. Tsang, N. Raza, B. S. Giri, D. Kukkar and K.-H. Kim, *ACS Appl. Mater. Interfaces*, 2018, **10**, 8797–8817.
129 J. Cao, M. Wang, H. Yu, Y. She, Z. Cao, J. Ye, A. M. Abd El-Aty, A. Hacımüftüoğlu, J. Wang and S. Lao, *J. Agric. Food Chem.*, 2020, **68**, 7298–7315.
130 N. Li, X. Wang, J. Chen, L. Sun and P. Chen, *2D Mater.*, 2015, **2**, 34018.
131 J. Peng, W. Yin, J. Shi, X. Jin and G. Ni, *Microchim. Acta*, 2019, **186**, 1–9.
132 J. Li, Y. Weng, C. Shen, J. Luo, D. Yu and Z. Cao, *Anal. Methods*, 2021, **13**, 2981–2988.
133 J. Hou, J. Dong, H. Zhu, X. Teng, S. Ai and M. Mang, *Biosens. Bioelectron.*, 2015, **68**, 20–26.
134 X. Yan, H. Li, X. Wang and X. Su, *Talanta*, 2015, **131**, 88–94.
135 M. M. F. Chang, I. R. Ginjom and S. M. Ng, *Sens. Actuators, B*, 2017, **242**, 1050–1056.
136 Y. Hu, J. Li and X. Li, *Anal. Bioanal. Chem.*, 2019, **411**, 7879–7887.
137 K. Zhang, Q. Mei, G. Guan, B. Liu, S. Wang and Z. Zhang, *Anal. Chem.*, 2010, **82**, 9579–9586.
138 X. Dou, X. Chu, W. Kong, J. Luo and M. Yang, *Anal. Chim. Acta*, 2015, **891**, 291–297.
139 A. K. K. Bhasin, P. Raj, P. Chauhan, S. K. Mandal, S. Chaudhary, N. Singh and N. Kaur, *New J. Chem.*, 2020, **44**, 3341–3349.
140 R. M. Abdelhameed, M. El-Naggar, M. Taha, S. Nabil, M. A. Youssef, N. S. Awwad and M. T. El Sayed, *J. Mol. Struct.*, 2020, **1199**, 127000.
141 Q. Chen, R. Sheng, P. Wang, Q. Ouyang, A. Wang, S. Ali, M. Zareef and M. M. Hassan, *Spectrochim. Acta, Part A*, 2020, **241**, 118654.
142 H. A. Azab, A. S. Orabi and A. M. Abbas, *J. Lumin.*, 2015, **160**, 181–187.
143 M. Wang, K. Su, J. Cao, Y. She, A. M. Abd El-Aty, A. Hacımüftüoğlu, J. Wang, M. Yan, S. Hong and S. Lao, *Talanta*, 2019, **192**, 295–300.
144 S.-H. Hung, J.-Y. Lee, C.-C. Hu and T.-C. Chiu, *Food Chem.*, 2018, **260**, 61–65.
145 C.-W. Hsu, Z.-Y. Lin, T.-Y. Chan, T.-C. Chiu and C.-C. Hu, *Food Chem.*, 2017, **224**, 353–358.
146 Z. Sheng, J. Zhang, C. Li and L. Chen, *Anal. Methods*, 2016, **8**, 8506–8513.
147 S. Li, J. Luo, G. Yin, Z. Xu, Y. Le, X. Wu, N. Wu and Q. Zhang, *Sens. Actuators, B*, 2015, **206**, 14–21.
148 Z. Cui, C. Han and H. Li, *Analyst*, 2011, **136**, 1351–1356.
149 Y. Shen, F. Yan, X. Huang, X. Zhang, Y. Zhang, C. Zhang, J. Jin, H. Li and S. Yao, *RSC Adv.*, 2016, **6**, 88096–88103.
150 W. Bai, G. Qin, J. Wang, L. Li and Y. Ni, *Dyes Pigm.*, 2021, **193**, 109473.
151 Q. Sun, Q. Yao, Z. Sun, T. Zhou, D. Nie, G. Shi and L. Jin, *Chin. J. Chem.*, 2011, **29**, 2134–2140.
152 Q. Long, H. Li, Y. Zhang and S. Yao, *Biosens. Bioelectron.*, 2015, **68**, 168–174.
153 J. Tang and L. Xiang, *Pol. J. Environ. Stud.*, 2016, **25**, 787–793.
154 W. Song, H.-J. Zhang, Y.-H. Liu, C.-L. Ren and H.-L. Chen, *Chin. Chem. Lett.*, 2017, **28**, 1675–1680.
155 X. Yan, H. Li, Y. Yan and X. Su, *Food Chem.*, 2015, **173**, 179–184.
156 X. Hu, F. Wang, Q. Peng, J. Hu, H. Peng, L. Li, B. Zheng, J. Du and D. Xiao, *RSC Adv.*, 2019, **9**, 13048–13053.

157 X. Xu, Y. Guo, X. Wang, W. Li, P. Qi, Z. Wang, X. Wang, S. Gunasekaran and Q. Wang, *Sens. Actuators, B*, 2018, **260**, 339–345.
158 K. He, Z. Li, L. Wang, Y. Fu, H. Quan, Y. Li, X. Wang, S. Gunasekaran and X. Xu, *ACS Appl. Mater. Interfaces*, 2019, **11**, 26250–26260.
159 K. Kanagaraj, A. Affrose, S. Sivakolunthu and K. Pitchumani, *Biosens. Bioelectron.*, 2012, **35**, 452–455.
160 H. A. Azab, G. M. Khairy and R. M. Kamel, *Spectrochim. Acta, Part A*, 2015, **148**, 114–124.
161 F. Yao, Y. Sun, C. Tan, S. Wei, X. Zhang, X. Hu and J. Fan, *J. Korean Chem. Soc.*, 2011, **55**, 932–935.
162 X. Ren, H. Liu and L. Chen, *Microchim. Acta*, 2015, **182**, 193–200.
163 F. Ashrafi Tafreshi, Z. Fatahi, S. F. Ghasemi, A. Taherian and N. Esfandiari, *PLoS One*, 2020, **15**, e0230646.
164 M. Arvand and A. A. Mirroshandel, *Food Chem.*, 2019, **280**, 115–122.
165 I. A. Ibrahim, A. M. Abbas and H. M. Darwish, *Luminescence*, 2017, **32**, 1541–1546.
166 Y. Lü, Q. Sun, B. Hu, X. Chen, R. Miao and Y. Fang, *New J. Chem.*, 2016, **40**, 1817–1824.
167 G. Kaur, A. Singh, A. Singh, N. Kaur and N. Singh, *Dalton Trans.*, 2018, **47**, 5595–5606.
168 J. Guan, J. Yang, Y. Zhang, X. Zhang, H. Deng, J. Xu, J. Wang and M.-S. Yuan, *Talanta*, 2021, **224**, 121834.
169 B. C. M. A. Ashwin, C. Saravanan, T. Stalin, P. Muthu Mareeswaran and S. Rajagopal, *ChemPhysChem*, 2018, **19**, 2768–2775.
170 J. Hou, X. Wang, S. Lan, C. Zhang, C. Hou, Q. He and D. Huo, *Anal. Methods*, 2020, **12**, 4130–4138.
171 L. Wang, Y. Bi, J. Hou, H. Li, Y. Xu, B. Wang, H. Ding and L. Ding, *Talanta*, 2016, **160**, 268–275.
172 Q. Yang, J. Wang, X. Chen, W. Yang, H. Pei, N. Hu, Z. Li, Y. Suo, T. Li and J. Wang, *J. Mater. Chem. A*, 2018, **6**, 2184–2192.
173 J. Guo, Y. Zhang, Y. Luo, F. Shen and C. Sun, *Talanta*, 2014, **125**, 385–392.
174 C.-X. Yu, F.-L. Hu, J.-G. Song, J.-L. Zhang, S.-S. Liu, B.-X. Wang, H. Meng, L.-L. Liu and L.-F. Ma, *Sens. Actuators, B*, 2020, **310**, 127819.
175 F. Zhang, X. Cao, D. Tian and H. Li, *Chin. J. Chem.*, 2015, **33**, 368–372.
176 Q. Wang, Q. Yin, Y. Fan, L. Zhang, Y. Xu, O. Hu, X. Guo, Q. Shi, H. Fu and Y. She, *Talanta*, 2019, **199**, 46–53.
177 M. Roth, R. H. Richards, D. P. Dobson and G. H. Rae, *Aquaculture*, 1996, **140**, 217–239.
178 V. Scognamiglio, G. Rea, F. Arduini and G. Palleschi, *Biosensors for sustainable food-new opportunities and technical challenges*, Elsevier, 2016.
179 S. Patel and S. Sangeeta, *Environ. Sci. Pollut. Res.*, 2019, **26**, 91–100.
180 T. M. B. F. Oliveira, M. F. Barroso, S. Morais, P. de Lima-Neto, A. N. Correia, M. B. P. P. Oliveira and C. Delerue-Matos, *Talanta*, 2013, **106**, 137–143.
181 B. Tiwari, S. Kharwar and D. N. Tiwari, *Cyanobacteria*, Elsevier, 2019, pp. 303–325.
182 A. K. Ghosh and M. Brindisi, *J. Med. Chem.*, 2015, **58**, 2895–2940.
183 M. Kundu, P. Krishnan, R. K. Kotnala and G. Sumana, *Trends Food Sci. Technol.*, 2019, **88**, 157–178.
184 N. I. M. Fauzi, Y. W. Fen, N. A. S. Omar and H. S. Hashim, *Sensors*, 2021, **21**, 3856.
185 T. M. B. F. Oliveira, F. W. P. Ribeiro, C. P. Sousa, G. R. Salazar-Banda, P. de Lima-Neto, A. N. Correia and S. Morais, *TrAC, Trends Anal. Chem.*, 2020, **124**, 115779.
186 N. L. Mdeni, A. O. Adeniji, A. I. Okoh and O. O. Okoh, *Molecules*, 2022, **27**, 618.
187 J. Dai, Y. Zhao, Y. Hou, G. Zhong, R. Gao, J. Wu, B. Shen and X. Zhang, *Dyes Pigm.*, 2021, **192**, 109444.
188 C. Ma, J. Wu, W. Sun, Y. Hou, G. Zhong, R. Gao, B. Shen and H. Huang, *Sens. Actuators, B*, 2020, **325**, 128798.
189 D. Liu, W. Chen, J. Wei, X. Li, Z. Wang and X. Jiang, *Anal. Chem.*, 2012, **84**, 4185–4191.
190 S. Qian and H. Lin, *Anal. Chem.*, 2015, **87**, 5395–5400.
191 Y. Chen, X. Qin, C. Yuan, R. Shi and Y. Wang, *Dyes Pigm.*, 2020, **181**, 108529.
192 D. Zhao, C. Chen, J. Sun and X. Yang, *Analyst*, 2016, **141**, 3280–3288.
193 C. Zhang, H. Cui, J. Cai, Y. Duan and Y. Liu, *J. Agric. Food Chem.*, 2015, **63**, 4966–4972.
194 F. Shahdost-Fard, N. Fahimi-Kashani and M. R. Hormozi-Nezhad, *Talanta*, 2021, **221**, 121467.
195 N. Saleh and N. A. F. Al-Rawashdeh, *J. Fluoresc.*, 2006, **16**, 487–493.
196 M. Del Pozo, L. Hernández and C. Quintana, *Talanta*, 2010, **81**, 1542–1546.
197 Y. Yang, D. Huo, H. Wu, X. Wang, J. Yang, M. Bian, Y. Ma and C. Hou, *Sens. Actuators, B*, 2018, **274**, 296–303.
198 R. V. Nair, R. T. Thomas, A. P. Mohamed and S. Pillai, *Microchem. J.*, 2020, **157**, 104971.
199 J.-C. Wei, B. Wei, W. Yang, C.-W. He, H.-X. Su, J.-B. Wan, P. Li and Y.-T. Wang, *Food Chem. Toxicol.*, 2018, **119**, 430–437.
200 C. Zhang, K. Zhang, T. Zhao, B. Liu, Z. Wang and Z. Zhang, *Sens. Actuators, B*, 2017, **252**, 1083–1088.
201 Z. Tang, Z. Chen, G. Li and Y. Hu, *Anal. Chim. Acta*, 2020, **1136**, 72–81.
202 X.-X. Peng, G.-M. Bao, Y.-F. Zhong, L. Zhang, K.-B. Zeng, J.-X. He, W. Xiao, Y.-F. Xia, Q. Fan and H.-Q. Yuan, *Food Chem.*, 2021, **343**, 128504.
203 Y. Huang, J. Wang, S.-F. Xue, Z. Tao, Q.-J. Zhu and Q. Tang, *J. Inclusion Phenom. Macrocyclic Chem.*, 2012, **72**, 397–404.
204 Z. Wang, L. Wu, B. Shen and Z. Jiang, *Talanta*, 2013, **114**, 124–130.
205 J. Xu, L. DU, W. U. Hao, W. WU and Y. CHANG, *J. Integr. Agric.*, 2012, **11**, 1861–1870.
206 X. Zeng, J. Ma, L. Luo, L. Yang, X. Cao, D. Tian and H. Li, *Org. Lett.*, 2015, **17**, 2976–2979.
207 M.-H. Tseng, C.-C. Hu and T.-C. Chiu, *Dyes Pigm.*, 2019, **171**, 107674.
208 H. Li and F. Qu, *Chem. Mater.*, 2007, **19**, 4148–4154.
209 N. L. Pacioni and A. V. Veglia, *Anal. Chim. Acta*, 2007, **583**, 63–71.

210 T. Ogoshi and A. Harada, *Sensors*, 2008, **8**, 4961–4982.
211 Y. Fan, L. Liu, D. Sun, H. Lan, H. Fu, T. Yang, Y. She and C. Ni, *Anal. Chim. Acta*, 2016, **916**, 84–91; X. Kang, J. Yuan, X. Gu, X. Li, T. Wen, M. He, Y. He, X. Yang and Y. Li, *ACS Appl. Nano Mater.*, 2025, **8**, 1663–1672.
212 Y. Chen, J. Lai, M. Zhang, T. Zhao, S. Wang, J. Li and S. Liu, *Food Sci.*, 2022, **43**, 285–292.
213 X. Liu, Q. Zhang, S. Li, P. Mi, D. Chen, X. Zhao and X. Feng, *Chemosphere*, 2018, **199**, 16–25.
214 I. Bragança, P. C. Lemos, P. Barros, C. Delerue-Matos and V. F. Domingues, *Sci. Total Environ.*, 2018, **619**, 685–691.
215 I. Bragança, A. P. Mucha, M. P. Tomasino, F. Santos, P. C. Lemos, C. Delerue-Matos and V. F. Domingues, *Chemosphere*, 2019, **220**, 1179–1186.
216 X. Zhang, T. Zhang, X. Ren, X. Chen, S. Wang and C. Qin, *Front. Endocrinol.*, 2021, **12**, 656106.
217 E. T. Knapke, D. de P. Magalhaes, M. A. Dalvie, D. Mandrioli and M. J. Perry, *Toxicology*, 2022, **465**, 153017.
218 J. Wang, L. Gao, D. Han, J. Pan, H. Qiu, H. Li, X. Wei, J. Dai, J. Yang and H. Yao, *J. Agric. Food Chem.*, 2015, **63**, 2392–2399.
219 L. Gao, X. Li, Q. Zhang, J. Dai, X. Wei, Z. Song, Y. Yan and C. Li, *Food Chem.*, 2014, **156**, 1–6.
220 C. Liu, Z. Song, J. Pan, X. Wei, L. Gao, Y. Yan, L. Li, J. Wang, R. Chen and J. Dai, *J. Phys. Chem. C*, 2013, **117**, 10445–10453.
221 X. Wei, T. Hao, Y. Xu, K. Lu, H. Li, Y. Yan and Z. Zhou, *RSC Adv.*, 2015, **5**, 79511–79518.
222 H. Li, Y. Li and J. Cheng, *Chem. Mater.*, 2010, **22**, 2451–2457.
223 J. Wang, H. Qiu, H. Shen, J. Pan, X. Dai, Y. Yan, G. Pan and B. Sellergren, *Biosens. Bioelectron.*, 2016, **85**, 387–394.
224 X. Wei, T. Hao, Y. Xu, K. Lu, H. Li, Y. Yan and Z. Zhou, *Sens. Actuators, B*, 2016, **224**, 315–324.
225 X. Ren and L. Chen, *Biosens. Bioelectron.*, 2015, **64**, 182–188.
226 X. Li, H.-F. Jiao, X.-Z. Shi, A. Sun, X. Wang, J. Chai, D.-X. Li and J. Chen, *Biosens. Bioelectron.*, 2018, **99**, 268–273.
227 H. Li, X. Wei, Y. Xu, K. Lu, Y. Zhang, Y. Yan and C. Li, *J. Alloys Compd.*, 2017, **705**, 524–532.
228 L. Gao, W. Han, Y. Yan, X. Li, C. Li and B. Hu, *Anal. Methods*, 2016, **8**, 2434–2440.
229 Y. Zhang, X. Zhu, M. Li, H. Liu and B. Sun, *J. Agric. Food Chem.*, 2022, **70**, 6059–6071.
230 X. Zhu, L. Han, H. Liu and B. Sun, *Food Chem.*, 2022, **379**, 132154.
231 D. Zhang, J. Tang and H. Liu, *Anal. Bioanal. Chem.*, 2019, **411**, 5309–5316.
232 Q. Wang, J. Jiang, W. Sui, X. Lin and B. Liu, *Anal. Lett.*, 2017, **50**, 1139–1149.
233 S. Ge, J. Lu, L. Ge, M. Yan and J. Yu, *Spectrochim. Acta, Part A*, 2011, **79**, 1704–1709.
234 Y. Cai, X. He, P. L. Cui, W. Z. Yuan, J. P. Wang and J. Liu, *Food Chem.*, 2020, **319**, 126539.
235 T. Qin, X. Zhao, C. Song, T. Lv, S. Chen, Z. Xun, Z. Xu, Z. Zhang, H. Xu and C. Zhao, *Chem. Eng. J.*, 2023, **451**, 139022.
236 F. Fang, Q. Zhao, R. Fan, H. Wang, J. Zhu and X. Wang, *Microchem. J.*, 2022, **172**, 106954.
237 J. Shah, M. Rasul Jan, B. Ara and F.-N. Shehzad, *Environ. Monit. Assess.*, 2011, **178**, 111–119.
238 M. Majd and S. Nojavan, *Microchim. Acta*, 2021, **188**, 1–12.
239 A. Amiri, M. Baghayeri and M. Sedighi, *Microchim. Acta*, 2018, **185**, 1–9.
240 S. Wang, Y. She, S. Hong, X. Du, M. Yan, Y. Wang, Y. Qi, M. Wang, W. Jiang and J. Wang, *J. Hazard. Mater.*, 2019, **367**, 686–693.
241 S. Zoughi, F. Faridbod, A. Amiri and M. R. Ganjali, *Food Chem.*, 2021, **350**, 129197.
242 S. Mohapatra, M. K. Bera and R. K. Das, *Sens. Actuators, B*, 2018, **263**, 459–468.
243 D. Sahoo, A. Mandal, T. Mitra, K. Chakraborty, M. Bardhan and A. K. Dasgupta, *J. Agric. Food Chem.*, 2018, **66**, 414–423.
244 S. A. Nsibande and P. B. C. Forbes, *Luminescence*, 2019, **34**, 480–488.
245 H. Su, L. Chen, B. Sun and S. Ai, *Sens. Actuators, B*, 2012, **174**, 458–464.
246 G. Liu, T. Li, X. Yang, Y. She, M. Wang, J. Wang, M. Zhang, S. Wang, F. Jin and M. Jin, *Carbohydr. Polym.*, 2016, **137**, 75–81.
247 S. Halder, A. Barma, C. Rizzoli, P. Ghosh and P. Roy, *ACS Appl. Nano Mater.*, 2019, **2**, 5469–5474.
248 V. Romero, S. P. S. Fernandes, P. Kovář, M. Pšeničkа, Y. V. Kolen'ko, L. M. Salonen and B. Espiña, *Microporous Mesoporous Mater.*, 2020, **307**, 110523.
249 M. Amjadi and R. Jalili, *Biosens. Bioelectron.*, 2017, **96**, 121–126.
250 Q. Yu, C. He, Q. Li, Y. Zhou, N. Duan and S. Wu, *Microchim. Acta*, 2020, **187**, 1–10.
251 Y. Fan, R.-H. Gao, Y. Huang, B. Bian, Z. Tao and X. Xiao, *Front. Chem.*, 2019, **7**, 154.
252 Q. Li, S.-C. Qiu, J. Zhang, K. Chen, Y. Huang, X. Xiao, Y. Zhang, F. Li, Y.-Q. Zhang and S.-F. Xue, *Org. Lett.*, 2016, **18**, 4020–4023.
253 S. Walia and A. Acharya, *J. Nanopart. Res.*, 2014, **16**, 1–10.
254 Y. Yang, A. Han, S. Hao, X. Li, X. Luo, G. Fang, J. Liu and S. Wang, *Analyst*, 2020, **145**, 6683–6690.
255 H.-F. Wang, Y. He, T.-R. Ji and X.-P. Yan, *Anal. Chem.*, 2009, **81**, 1615–1621.
256 M. Yang, A. Han, J. Duan, Z. Li, Y. Lai and J. Zhan, *J. Hazard. Mater.*, 2012, **237**, 63–70.
257 Q. Liu, K. Wang, J. Huan, G. Zhu, J. Qian, H. Mao and J. Cai, *Analyst*, 2014, **139**, 2912–2918.
258 M. Jia, Z. Zhang, J. Li, H. Shao, L. Chen and X. Yang, *Sens. Actuators, B*, 2017, **252**, 934–943.
259 Z. Zhang, X. Ma, B. Li, J. Zhao, J. Qi, G. Hao, R. Jianhui and X. Yang, *Analyst*, 2020, **145**, 963–974.
260 X. Wang, J. Yu, X. Wu, J. Fu, Q. Kang, D. Shen, J. Li and L. Chen, *Biosens. Bioelectron.*, 2016, **81**, 438–444.
261 S. Xu, Y. Zou and H. Zhang, *Talanta*, 2020, **211**, 120711.
262 N. Xu, Q. Zhang, B. Hou, Q. Cheng and G. Zhang, *Inorg. Chem.*, 2018, **57**, 13330–13340.
263 N. Xu, Q. Zhang and G. Zhang, *Dalton Trans.*, 2019, **48**, 2683–2691.

264 X.-Y. Guo, Z.-P. Dong, F. Zhao, Z.-L. Liu and Y.-Q. Wang, *New J. Chem.*, 2019, **43**, 2353–2361.
265 C.-L. Tao, B. Chen, X.-G. Liu, L.-J. Zhou, X.-L. Zhu, J. Cao, Z.-G. Gu, Z. Zhao, L. Shen and B. Z. Tang, *Chem. Commun.*, 2017, **53**, 9975–9978.
266 X.-Q. Wang, D.-D. Feng, J. Tang, Y.-D. Zhao, J. Li, J. Yang, C. K. Kim and F. Su, *Dalton Trans.*, 2019, **48**, 16776–16785.
267 J. Chi, B. Zhong, Y. Li, P. Shao, G. Liu, Q. Gao and B. Chen, *Z. Anorg. Allg. Chem.*, 2021, **647**, 1284–1293.
268 D. Feng, J. Tang, J. Yang, X. Ma, C. Fan and X. Wang, *J. Mol. Struct.*, 2020, **1221**, 128841.
269 P. Sharma, M. Kumar and V. Bhalla, *ACS Omega*, 2020, **5**, 19654–19660.
270 F. Wang, X. Zhang, C. Huangfu, M. Zhu, C. Li and L. Feng, *Food Chem.*, 2022, **370**, 131033.
271 L. Fan, F. Wang, D. Zhao, X. Sun, H. Chen, H. Wang and X. Zhang, *Spectrochim. Acta, Part A*, 2020, **239**, 118467.
272 B. Lin, Y. Yu, R. Li, Y. Cao and M. Guo, *Sens. Actuators, B*, 2016, **229**, 100–109.
273 J. Guo, Y. Li, L. Wang, J. Xu, Y. Huang, Y. Luo, F. Shen, C. Sun and R. Meng, *Anal. Bioanal. Chem.*, 2016, **408**, 557–566.
274 W. Hu, Q. Chen, H. Li, Q. Ouyang and J. Zhao, *Biosens. Bioelectron.*, 2016, **80**, 398–404.
275 L. Yang, H. Sun, X. Wang, W. Yao, W. Zhang and L. Jiang, *Microchim. Acta*, 2019, **186**, 1–11.
276 X. Yan, H. Li, Y. Li and X. Su, *Anal. Chim. Acta*, 2014, **852**, 189–195.
277 M. P. Shirani, B. Rezaei and A. A. Ensafi, *Spectrochim. Acta, Part A*, 2019, **210**, 36–43.
278 F. Qu, X. Zhou, J. Xu, H. Li and G. Xie, *Talanta*, 2009, **78**, 1359–1363.
279 W. Lei, Z. Gu, W. Si, F. Wang and Q. Hao, *J. Electrochem. Soc.*, 2013, **160**, H502.
280 J. Liu, W. H. Xiong, L. Y. Ye, W. S. Zhang and H. Yang, *J. Agric. Food Chem.*, 2020, **68**, 5572–5578.
281 Y. Liu, N. Cao, W. Gui and Q. Ma, *Talanta*, 2018, **183**, 339–344.